

This is an Open Access document downloaded from ORCA, Cardiff University's institutional repository:<https://orca.cardiff.ac.uk/id/eprint/142486/>

This is the author's version of a work that was submitted to / accepted for publication.

Citation for final published version:

Alves, Tiago M. , Tugend, Julie, Holford, Simon, Bertoni, Claudia and Li, Wei 2021. Editorial: continental margins unleashed - from their early inception to continental breakup. *Marine and Petroleum Geology* 129 , 105097. 10.1016/j.marpetgeo.2021.105097

Publishers page: <https://www.sciencedirect.com/science/article/abs/...>

Please note:

Changes made as a result of publishing processes such as copy-editing, formatting and page numbers may not be reflected in this version. For the definitive version of this publication, please refer to the published source. You are advised to consult the publisher's version if you wish to cite this paper.

This version is being made available in accordance with publisher policies. See <http://orca.cf.ac.uk/policies.html> for usage policies. Copyright and moral rights for publications made available in ORCA are retained by the copyright holders.



1       **Editorial: Continental margins unleashed - From their**  
2                   **early inception to continental breakup**

3  
4                   Alves, T.M.<sup>1</sup>, Tugend, J.<sup>2,3</sup>, Holford, S.<sup>4</sup>, Bertoni, C.<sup>5</sup>, Li, W.<sup>6,7,8,9</sup>

5  
6   1-3D Seismic Laboratory, School of Earth and Ocean Sciences, Main Building-Park Place,  
7   Cardiff University, Cardiff CF 10 3AT, United Kingdom (corresponding author:  
8   alvest@cardiff.ac.uk)

9   2-Sorbonne Université, CNRS-INSU, Institut des Sciences de la Terre Paris, IStEP UMR  
10  7193, F-75005 Paris, France

11  3-Currently at CY Cergy Paris Université, GEC, F-95000, Cergy, France

12  4-Australian School of Petroleum and Energy Resources, University of Adelaide, Adelaide,  
13  Australia

14  5-Department of Earth Sciences, University of Oxford, South Parks Rd, Oxford, OX1 3AN,  
15  United Kingdom

16  6-CAS Key Laboratory of Ocean and Marginal Sea Geology, South China Sea Institute of  
17  Oceanology, Chinese Academy of Sciences, Guangzhou, 510301 China

18  7-Southern Marine Science and Engineering Guangdong Laboratory, Guangzhou, 511458  
19  China

20 8-Innovation Academy of South China Sea Ecology and Environmental Engineering, Chinese  
21 Academy of Sciences, Guangzhou, 510301 China

22 9-University of Chinese Academy of Sciences, Beijing, 100049 China

23

24 **Keywords:** Continental margins; continental breakup; thermal evolution; salt tectonics;  
25 structures; sediments.

26

27

## 28 **Abstract**

29 It is clear from new state-of-the-art data that the processes responsible for  
30 ‘unleashing’ tectonic plates are distinct when moving across, and along, continental margins.  
31 There is simply no evolutionary sequence that applies to all continental margins, and even  
32 adjacent sedimentary basins on the same continental margins are known to record distinct  
33 geological processes during their formation. This is of key importance to characterise their  
34 economic potential as the last tectonic pulses that fully separate, or rift, distinct continents  
35 have the potential to affect the thermal and structural evolutions of the areas where  
36 continental margins will soon form. This Special Issue presents new data from economically  
37 significant areas of continental margins where exploration work is ongoing, or just started,  
38 not only in terms of their hydrocarbon potential, but also as hosts of water, geothermal and  
39 mineral resources. Contributions to the Special Issue vary from tackling local, but important,

40 sources of fluid in new frontier areas, to broad plate-scale geophysical modelling explaining  
41 continental breakup, or regional tectono-stratigraphic analysis of new frontier areas.

42

## 43 **1. Introduction**

44 Recent work has recognised the definition of ‘passive’ or ‘rifted’ margins as an  
45 oversimplification of a tectonic setting that is everything but ‘passive’ in the strict sense of  
46 the word. In fact, the distal margins of tectonic plates are now identified as preferential loci of  
47 magmatism, tectonism and complex mantle-crust processes at the time of continental breakup  
48 (Gillard et al., 2019; Lei et al., 2019; Lymer et al., 2019; Monteleone et al., 2019; Gallahue et  
49 al., 2020; Guan et al., 2019; Nirrengarten et al., 2020; Tugend et al., 2020). Often these same  
50 processes are renewed several millions of years after full breakup occurred between  
51 continents, or tectonic plates (Gillard et al., 2017; 2019; Epin et al., 2019; McDermott et al.,  
52 2019). Distal margins of tectonic plates can therefore record complex continental breakup,  
53 from relatively simple dip-slip extension to margin-perpendicular extension or a complex  
54 ‘unzip’ breakup in areas dominated by oblique rifting and local strike-slip movements  
55 (Ulvrova et al., 2019; Jerram et al., 2019). A key aspect seldom recognised on many a  
56 continental margin is that ridge push accompanies, or immediately follows, the continental  
57 breakup process, and is capable of controlling stress distribution on distal parts of continental  
58 margins well after these are formed (Doré et al., 2008; Alves and Cunha, 2018). Ultimately, a  
59 change from divergent to convergent geodynamic context during post-rift time may result in  
60 the formation of new convergent margins by initiating subduction at Ocean-Continent  
61 Transitions (OCT) zones of passive margins (Tugend et al., 2014; van Hinsbergen et al. 2019;  
62 McCarthy et al., 2020).

63 Economically, the aspects above are important because of their potential impact on the  
64 subsidence and thermal evolutions of continental margins. Originally grouped as ‘volcanic’  
65 or ‘non-volcanic’ (Mutter et al., 1988; White and McKenzie, 1989), the thermal evolution of  
66 continental margins is now recognised as obeying variable tectonic and magmatic  
67 interactions, which control their subsidence histories (Mutter, 1993). Because of the  
68 incredibly wide spectrum of observed geometries (Franke et al., 2013), researchers became  
69 increasingly aware that local geodynamic aspects can control the formation of distal, deep-  
70 water sedimentary basins.

71 Part of the rationale for compiling this Special Issue related to the urgent need of  
72 providing new information on these distal areas, where continental breakup occurred. In spite  
73 of an increasing number of recent studies focused on the stratigraphic and tectono-magmatic  
74 evolution related to continental breakup (e.g. Gillard et al., 2015; 2017; 2019; Peron-Pinvidic  
75 and Osmundsen, 2016; Tugend et al., 2020; Soares et al., 2012; Alves and Cunha, 2018;  
76 Alves et al., 2020) the interplay of geodynamic processes is not yet fully known for the  
77 phases preceding the separation of tectonic plates.

78

79 *a) Geodynamic processes at the larger, continental-margin scale*

80 The geodynamic processes behind continental rifting, breakup and subsequent tectonic  
81 reactivation are addressed for the southern part of the South China Sea by **Nirrengarten et**  
82 **al.** and **Bai et al.** and also for the Angola-Gabon margins by **Fernandez et al.** In parallel,  
83 **Nirrengarten et al.** use new data collected by IODP Expedition 367-368 to characterise the  
84 modes of extension and continental breakup at the conjugate SE-China-NW Palawan margin.

85 They recognise that lithospheric and basement heterogeneities induced a rifting style  
86 characterised by a series of highly thinned rift basins revealing extensional faulting soling out  
87 at various crustal levels. Final rifting in the late Eocene triggered decompression melting and  
88 subsequent mid-ocean ridge type magmatism, with thinned continental crust showing both  
89 deep intrusions and shallow extrusive rocks. Importantly, initial magmatic activity was  
90 concomitant with deformation of incipient oceanic crust by extensional faulting. **Bai et al.**  
91 move a step forward in our knowledge of SE Asia to show that the crustal stretching styles of  
92 the eastern margins of the South China Sea-Palawan conjugate are distinct. From  
93 approximately symmetric in the eastern margins, they become asymmetric in the western  
94 margins towards Vietnam. They further conclude that such asymmetry is due to post-rift  
95 lower crust flow and continental collision. Continuing this same theme, **Fernandez et al.**  
96 prove, for the South Atlantic Margin, that breakup volcanism is common along Angola and  
97 Gabon. Here, syn-breakup volcanism predates and is synchronous to the Aptian evaporites  
98 that seal sub-salt hydrocarbon prospects in West Africa. **Gómez-Romeu et al.** conclude on  
99 the minimum values of crustal extension necessary to trigger continental breakup offshore  
100 West Iberia based on gravity anomaly inversions, subsidence analyses, and fault heave  
101 measurements. They estimate that approximately 172 km of extension are required to achieve  
102 crustal breakup alone, and that an extension discrepancy at the scale of the whole conjugate  
103 Iberia-Newfoundland margin system is shown not to exist.

104 A second set of contributions devoted to geodynamic aspects of continental margins  
105 focused on regional tectonic aspects. **Bezerra et al.** presented an example of a continental  
106 margin dominated by wrench tectonics during its post-rift stage, a character that generated  
107 important structural traps due to local inversion. Tectonic episodes were prolonged in time

108 and associated with the Andean Orogeny and its constituent stages. Multi-directional  
109 extension is also documented for South Zealandia by **Barrier et al.** between Australia and  
110 what would later be New Zealand. The authors identified diverse, but coeval, directions of  
111 extension during Late Cretaceous rifting. As a result, three fault sets are parallel to spreading  
112 centres that define the present-day margins of Zealandia, and these same sets are also  
113 recognised across contemporaneous Late Cretaceous rift basins in Zealandia. **Benoit et al.**  
114 concluded on the effect of structural inheritance on continental rifting style. By developing a  
115 case-study from the north-western Pyrenees, France, they have identified alternating periods  
116 of tectonic ‘sag’ and enhanced extension that were controlled by underlying salt. Crustal  
117 thinning continued until the end of the Early Cretaceous to create large detachment faults.

118

119 *b) Regional seismic-stratigraphic studies*

120 Regional seismic-stratigraphic studies highlighting particular geodynamic episodes of  
121 margin formation are developed in this Special Issue by **Praxedes et al.** for SE Brazil’s Rio  
122 Grande Rise, **Fyhn et al.** for the Gulf of Tonkin in SE Asia, **Hassaan et al.** for the Barents  
123 Sea, Northern Norway, **Zastrozhnov et al.** for the Mid-Norwegian Sea, and **Walker et al.**  
124 once again for West Iberia. **Praxedes et al.** focuses on oceanic plateaus in the South Atlantic  
125 that were formed away from continents, but show a clear syn- to early post-breakup origin.  
126 They conclude that graben-like structures in the Rio Grande Rise reveal aborted rift basins.  
127 Here, extensional tectonics led to important magmatism, with volcanic islands emerging  
128 above sea level in the Eocene to increase the deposition of volcanic breccia and ash layers in  
129 adjacent extensional basins. After this volcanism ceased, thermal subsidence took place over  
130 the entire rise with intense erosion and sedimentation. Only the uppermost sedimentary layers

131 of the Rio Grande Rise (Miocene-Holocene) were deposited in pelagic conditions and later  
132 offset by sub-vertical normal faults. **Fyhn et al.** use the Gulf of Tonkin as a case-study of a  
133 SE Asian rift basin formed in the Eocene-Oligocene. Linking with the South China Sea to the  
134 south, the Gulf of Tonkin records the deposition of continental syn-rift strata within a marked  
135 strike-slip tectonic regime. Transpression and transtension makes the seismic-stratigraphic  
136 definition of systems tracts (pre-, syn- and post-rift units) hard to achieve, but allowed at the  
137 same time the formation of locally subsiding basins where lacustrine source rocks were  
138 accumulated. The formation of a deep lake during the rift development stage resulted in  
139 deposition of lacustrine source rocks measuring hundreds of meters in thickness at Bach  
140 Long Vi Island, but possibly also elsewhere in the study area analysed by **Fyhn et al.**

141 **Hassaan et al.** identified new Carboniferous grabens in the SE Norwegian Barents Sea.  
142 Carboniferous evaporites in this part of the Norwegian continental margin may cap earliest  
143 Carboniferous-Devonian and older hydrocarbon prospects in the region. **Hassaan et al.**  
144 mapped five evaporite bodies that taper the Carboniferous grabens. In the late Devonian, the  
145 region comprised a central structural high (Fedynsky High), and two depressions to the north  
146 and south, having subsequently experienced transtensional deformation during a late  
147 Devonian-early Carboniferous NE-SW extensional phase. Further south in the Central  
148 Norwegian Sea, **Zastrozhnov et al.** conclude that Early Cretaceous to Paleocene basin  
149 evolution is associated with episodic phases of extension separated by intermediate cooling  
150 phases. The development of sedimentary sub-basins was controlled, at the time, by old crustal  
151 blocks (“buffers”), while elevated crustal marginal plateaus were suggested to occur in the  
152 outer Møre and Vøring basins. In such a setting, observations do not support evidence for a  
153 large zone of exhumed upper mantle to have formed before magmatism and continental

154 breakup. Further south in the West Iberian-Newfoundland conjugate, **Walker et al.**  
155 demonstrate the presence of thick latest Triassic-earliest Jurassic evaporites offshore NW  
156 Iberia. They conclude that the evaporites, and Lower-Mid-Jurassic strata above, mark a rough  
157 N-S tectonic separation between the proximal Lusitanian and Porto Basins, with seaways  
158 developing between the Tethys and Boreal oceans. This implies that early Mesozoic rifting in  
159 West Iberia was capable of forming distinct (proximal and distal) sectors on a newly-formed  
160 area of crustal extension, and that a likely continental landmass existed to the west of the  
161 Jurassic seaway separating Newfoundland from Iberia.

162

163 *c) Magmatic processes during, and after, continental rifting*

164 Magmatic processes on continental margins were the focus of a third set of papers in  
165 this Special Issue. **Zhang et al.**, focusing on the southern part of the South China Sea (i.e., on  
166 the conjugate margin of South China), prove that most of the syn-rift fault activity in this area  
167 occurred up to 15.5 Ma. They also suggest that crustal extension continued until the  
168 termination of seafloor spreading. Rigid crustal blocks on the distal margin formed an  
169 atypical necking zone, without any developed detachment, resulting in rapid breakup and  
170 narrow and thin distal domain without noticeable hyperextension geometries. Important  
171 magmatism occurred at the end of the seafloor spreading stage in the southern South China  
172 Sea. **Yao et al.** develop a similar analysis for the East China Sea, and prove that intruded  
173 sills, dikes and volcanoes reflect Miocene-Holocene magmatism. The impact of sill intrusion  
174 on regional petroleum systems was deemed significant by **Yao et al.** as forced folds induced  
175 by magma are prospective traps. However, sill intrusion in the East China Sea is not a result  
176 of extension, being rather derived from material upwelling due to dehydration and/or small-

177 scale convection in a large mantle wedge above the stagnant Pacific slab. Following this  
178 same theme, **Maillard et al.** present a review of transfer zones in the Western Mediterranean  
179 Basin, and their importance as foci of magmatism. The Valencia and Liguro-Provençal basins  
180 are, in the Western Mediterranean, separated by transfer zones that were able to focus  
181 magmatism across their length. Narrow syn-rift grabens form, in this area, transtensional  
182 pull-apart basins along the largest fracture zones and helped the extrusion of magma during  
183 tectonic episodes. **Omosanya** further develops this theme under a context of tectonic  
184 inversion of the Norwegian Sea, to present the Nalfar Dome as a long-lived structure. First  
185 formed due to the forced emplacement of magma during continental breakup between  
186 Norway and Greenland, the Nalfar Dome was later reactivated to form intricate folds and  
187 reactivated faults during multiple stages of tectonism. **Kalani et al.** further expanded the  
188 analysis of the Norwegian margin to present a tectono-stratigraphic interpretation for the  
189 Barents Sea. Of importance to the area was the multistage deformation recorded by the  
190 Egersund Basin as a result of changes in the direction of extension from NW-SE through E-  
191 W to NE-SW. Such changes involved dextral strike-slip movements and was to a varying  
192 degree influenced by basement structures (i.e. structural configuration and fabric), of a likely  
193 Proterozoic and Caledonian origin.

194

195 *d) Depositional systems of deep-water continental margins*

196 Geological aspects of specific sedimentary basins, and resource estimates for particular  
197 continental margins, were provided by five other articles in this Special Issue. **Chima et al.**  
198 develop a seismic-stratigraphic analysis of one of the most hydrocarbon-rich area in Africa,  
199 the Niger Delta offshore Southwest Nigeria. They analyse the western part of the Niger Delta

200 to find it forming during the Chattian (latest Oligocene), while the present-day channel-levee  
201 depositional systems were set in the Pliocene-Pleistocene. Prior to that, pounded slope basins  
202 were filled by amalgamated channel-level systems, while post-Pliocene strata reveal a  
203 predominance of erosional channels and mass-transport deposits. **Li et al.** continue along the  
204 lines of the previous article to conclude on the effect of slope instability in submarine channel  
205 initiation. They find that downslope and along-slope processes controlled the morphology of  
206 the headwall regions of a channel system in the South China Sea. Erosive channels were  
207 initiated after the formation of the Baiyun Slide Complex, a major landslide of Quaternary  
208 age (0.79 Ma and ~0.54 Ma). Importantly, a reversal in the importance of alongslope vs.  
209 downslope sedimentary processes was recorded after the scar of the Bayun Slide Complex  
210 was formed, i.e. the first incision of submarine channels marks the intensification of  
211 downslope sedimentary processes (e.g. turbidity currents and mass wasting) over alongslope  
212 processes. Similar downslope depositional processes dominate the Cenozoic evolution of  
213 Equatorial Brazil.

214 **Oliveira et al.** analyse deep-water depositional systems in the Ceará Basin, Equatorial  
215 Brazil, to conclude that mixed turbidite (cross-slope) depositional systems meet areas of the  
216 margin with important magmatism, generating atypical petroleum systems. Despite being part  
217 of a continental margin dominated by strike-slip tectonics since its inception, not obeying the  
218 common models explaining the formation of continental margins (Franke et al., 2011; Péron-  
219 Pinvidic et al., 2019), the Ceará Basin comprises aspects typically found on magma-rich (or  
220 volcanic) passive margins. They justify their assertion by stressing aspects of Ceará that are  
221 typical of volcanic margins: a) the presence of rift basins filled by volcanics (seaward dipping  
222 reflectors), b) the absence of exhumed mantle between the continental crust and oceanic

223 crust, c) the large presence of igneous intrusions, d) and the presence of a LIP in the Brazilian  
224 Equatorial Margin. **Almeida et al.** further conclude on the petroleum system(s) offshore  
225 Ceará based on the analysis of new data from productive oil fields: Curimã and Espada. Their  
226 comparison with oil and gas prospects on the conjugate margin of West Africa reveals the  
227 common aspects in Equatorial Brazil that enhance its potential has a hydrocarbon-rich region.  
228 In more detail, Almeida et al. show that combined traps on footwall blocks are successful  
229 plays near the shelf break of the Mundaú sub-basin, in similarity with the prolific Espoir and  
230 Baobab fields in Ivory Coast. Turbidite sands in drift units are also similar to those of the  
231 Stabroek block in Guyana and prospects in the Gulf of Guinea.

232

233 *e) Near-seafloor fluid migration*

234 Contributions to the Special Issue were first focused on explaining particular aspects of  
235 continental margins. Fluid migration and subsequent seafloor features documenting such a  
236 migration were presented by **Micallef et al.** for tectonically-controlled scarps offshore Malta.  
237 In this case study, the authors show how the reactivation of faults under extensional to  
238 transtensional stress regimes, occurring for the past 20 ka, has been responsible for the  
239 degassing of CH<sub>4</sub> and CO<sub>2</sub> on the sea floor. Pull-apart basins were formed and bounded by  
240 permeable onshore and offshore faults that have been active recently and simultaneously. A  
241 similar approach was followed by **Roelofse et al.**, for a region dominated by salt tectonics. In  
242 the East Breaks region of the Gulf of Mexico, USA, **Roelofse et al.**, demonstrate that shallow  
243 gas reservoirs are able to feed pockmarks on the sea floor, while deep reservoirs feed mud  
244 volcanoes and larger fluid-escape features located on the steepest flanks of salt structures.

245 The sizes of fluid-escape features were therefore shown to identify the relative depth of fluid  
246 sources in the Gulf of Mexico.

247 Shifting the focus to Eastern and Southeast Brazil, **Szatmari et al.** develop a  
248 comprehensive analysis of Aptian salt (and seal) units capping prolific sub-salt plays.  
249 Comprising some of the largest oil fields in the world, sub-salt reservoirs in Brazil show  
250 characteristics that depend in great part on the nature and deformation styles of sealing salt  
251 units above. **Szatmari et al.** provide depositional facies interpretation of the Brazilian salt  
252 giant using microscopy, cores, geologic sections and structural data from onshore salt mines.  
253 They postulate that local sources of excess Ca further increased the high Ca/Mg and low  
254 Ca/SO<sub>4</sub> ratios of Cretaceous seawater, favouring evaporite deposition. The lake brine was  
255 also altered by intense hydrothermal activity due to pre-salt mafic lava flows in the  
256 underlying rift sequence, of which the youngest are of 115 Ma, and also by percolation of  
257 seawater into the brine lake at depth across the proto-Walvis Ridge. In such a setting,  
258 seawater percolated into the South Atlantic simultaneously from the north and south.

259

### 260 **3. Studying the structure of distal passive margins to unleash continental breakup**

261 Continental breakup records the change from extension and thinning of continental  
262 lithosphere during rifting to the stable self-sustained accretion of oceanic lithosphere (Falvey,  
263 1974; Heezen, 1960; McKenzie, 1978). During continental breakup, the interaction of  
264 geodynamic processes operating in the heterogeneous continental lithosphere is recorded  
265 within the so-called Ocean-Continent Transition (OCT) zones of distal passive margins.  
266 Initially believed to be an instantaneous event, continental breakup is now often considered as

267 a transient phase of the life of passive margins obeying variable tectonic and magmatic  
268 interplays remaining to be unleashed.

269 First defined as either “volcanic” or “non-volcanic” based on the interpreted  
270 occurrence, or apparent absence, of volcanic activity (Mutter et al., 1988; White and  
271 McKenzie, 1989), old classifications implied that rifting and continental breakup at divergent  
272 margins were either controlled by magmatic or tectonic processes (Mutter, 1993). New data  
273 provided a new look into old classifications; evidence of significant tectonic activity has been  
274 reported from “volcanic” passive margins at the time of continental breakup (e.g., Skogseid  
275 and Eldhom, 1989; Skogseid, 2001). In parallel, Ocean Drilling Program (ODP) expeditions  
276 on “non-volcanic” passive margins have recovered magmatic rocks in the OCT, as was the  
277 case of ODP Sites 1068 and 1070 across the Iberia margin (Whitmarsh et al., 1998) and ODP  
278 Site 1277 across the Newfoundland margin (Tucholke et al., 2004). Divergent, or rifted  
279 margins are now commonly referred to as “magma-poor” or “magma-rich” (Sawyer et al.,  
280 2007) using a series of morphological features considered as characteristic of the OCT of one  
281 or the other end-member archetypes (e.g., Franke et al., 2013; Doré and Lundin, 2015). In  
282 spite of the incredibly wide spectrum of observed OCT geometries differing from these end-  
283 member archetypes, the use of this terminology acknowledges the importance given to  
284 magmatic processes in breaking up continents (Buck, 2004; Keir, 2014).

285 Magma-rich rifted margins are often interpreted as formed by the interaction of a  
286 thinning, rifting crust/upper mantle with a Large Igneous Province (Coffin and Eldhom,  
287 1994). The spatial and temporal relationships between LIP emplacement and rifting are  
288 complex (e.g. Stica et al., 2014), impacting the magmatic production during continental  
289 breakup (Skogseid, 2001). When magma is produced in significant volumes, reflection

290 seismic data can often image the presence of Seaward Deeping Reflectors (SDR) at the OCT  
291 (Fig. 1, Hinz, 1981), corresponding to extrusive basaltic lava flows emplaced in sub-aerial  
292 conditions in the places where they were drilled, e.g. by DSDP Leg 81 off the British Isles  
293 (Roberts et al., 1984), by ODP Leg 104 offshore Norway (Eldholm et al., 1987; 1989), and by  
294 ODP Legs 152 and 163 offshore Greenland (Duncan et al., 1996; Larsen and Saunders, 1998;  
295 Larsen et al., 1994). Other geophysical data such as refraction profiles or gravity models  
296 reveal the occurrence of high velocity bodies at depth, together with the SDRs, features that  
297 are interpreted as the intrusive magmatic counterpart of these same SDRs (White and  
298 McKenzie, 1989; Menzies et al., 2002). High-velocity bodies partly intrude the lower  
299 continental crust at the OCT (White et al., 2008), but the nature of the crust below the SDRs  
300 remains controversial as it is difficult to unambiguously constrain.

301         Several hypotheses are possible depending on the rift configuration prior to continental  
302 breakup. For example, by reassessing the structure and protracted tectono-magmatic  
303 evolution of the mid-Norwegian rifted margin, **Zastrozhnov et al.** (this issue) show that  
304 magma-rich continental breakup during the Paleogene was partly controlled by deep-seated  
305 structural highs previously formed during the Mesozoic rifting of the Møre and Vøring  
306 basins. The intensity of the magmatic activity at breakup time controlled the complex  
307 subsidence history of the area studied by **Zastrozhnov et al.**, as also documented on other  
308 magma-rich margins where uplift and inversion of adjacent rift basins can be observed  
309 (Skogseid et al., 2000). The thermal evolution of such margins remains to be further  
310 investigated, notably the effect of sills intrusions in rift basins and their effect on ‘atypical’  
311 petroleum systems, as discussed by **Oliveira et al.** (this issue). Magma-rich rifted margins  
312 generally record an early onset of decompression melting and melt extraction during crustal

313 thinning (Menzies et al., 2002; Tugend et al., 2020) but that does not mean that continental  
314 breakup is solely driven by magmatic processes.

315       Even though the formation mechanisms of SDRs remain open (e.g. Buck 2017),  
316 analyses of SDR geometries conducted by more and more studies indicate that those  
317 emplaced during the earliest stage of continental breakup are fault controlled (McDermott et  
318 al., 2018; Harkin et al., 2020; Chauvet et al., 2020). Extensional shear zones have also been  
319 recognised in intruded lower continental crust adjacent to OCT, possibly accommodating  
320 syn-magmatic extensional deformation (Clerc et al., 2015; Geoffroy et al., 2015). An  
321 increasing number of studies show that extension at magma-rich rifted margins is not only  
322 accommodated by magmatic accretion; complex tectono-magmatic interplays also occur at  
323 the time of continental breakup and remain to be investigated.

324

325       Magma-poor margins record a late onset of melt extraction relative to lithosphere  
326 thinning and crustal separation, thus enabling the exhumation of upper mantle rocks in the  
327 OCT (Fig.1). The location and amount of magmatic products emplaced during rifting and  
328 continental breakup is often ambiguous on these margins (Tugend et al., 2020), explaining  
329 why they have long been referred to as “non-volcanic”. As a result, determining the modes  
330 and amount of extension accommodated by the continental lithosphere was given much more  
331 emphasis than magmatic processes on magma-poor margins. Because of the available drilling  
332 constraints and high-resolution seismic data, multiple studies have focussed on the Iberia-  
333 Newfoundland rifted margins to determine the extension required to achieve crustal rupture  
334 and separation; these studies have used section balancing (e.g., Ranero and Pérez-Gussinyé,  
335 2010), fault heave summation (e.g., Davis and Kusznir, 2004; Reston, 2005; Reston and

336 McDermott, 2015; Lymer et al., 2019), extension derived from crustal and lithosphere  
337 thinning (e.g., Davis and Kusznir, 2004), and kinematic forward modelling (Jeannot et al.,  
338 2016). An extension discrepancy is generally observed when applying different methods,  
339 notably between the measurements obtained from fault heave summation and the extension  
340 derived from crustal and lithosphere thinning (Reston, 2007).

341         The multi-method approach adopted by **Gomez-Romeu et al.** (this issue) enabled them  
342 to re-evaluate this apparent paradox for the Iberia-Newfoundland conjugate. They show that  
343 by taking into account previously unrecognized polyphase faulting (Reston, 2005; Reston and  
344 McDermott, 2015) and the rolling-hinge geometry of faults (e.g., Lymer et al., 2019),  
345 extension discrepancies are not recorded at the scale of the whole continental margin. To  
346 account for polyphase and rolling-hinge faulting is a complex task, nonetheless, as it is clear  
347 from new seismic data that the accommodation of extension on distal rifted margins results in  
348 different structural styles, including high-angle or low-angle extensional faults dipping either  
349 ocean- or continentwards (e.g., Gillard et al., 2016; Clerc et al., 2018). This variability  
350 depends on the initial rheological zoning of the continental lithosphere and its evolution  
351 during rifting (e.g., Reston and Pérez-Gussinyé, 2007). In such a setting, the onset of  
352 magmatic production and its extraction to the sea floor appear progressive in many magma-  
353 poor OCT (Desmurs et al., 2002; Jagoutz et al., 2007; Manatschal and Muntener 2009;  
354 Gillard et al., 2015; 2017; Peron-Pinvidic and Osmundsen 2016; Tugend et al., 2020). The  
355 interplay between hydration (i.e. serpentinization) and magmatic processes occurring in the  
356 exhumed mantle rocks during continental breakup (Perez-Gussinyé et al., 2001) also largely  
357 contributes to the complex structural style and polyphase evolution observed in some magma-  
358 poor OCTs (Fig. 1, Gillard et al., 2015; 2019). In turn, oceanward deepening of the soling

359 depth of faults can notably be interpreted as resulting from changes in basement rheology and  
360 composition with increasing melt production (Gillard et al., 2019). Hence, even if the amount  
361 of melt is difficult to evaluate, melt production and extraction are also key parameters to take  
362 into account to unravel the mechanisms of continental breakup at magma-poor rifted margins  
363 (e.g., Minshull et al., 2001; Whitmarsh et al., 2001; Pérez-Gussinyé et al., 2006; Fletcher et  
364 al., 2009; Muntener et al., 2010; Gillard et al., 2019; Tugend et al., 2020).

365 An important aspect proven in this Special Issue is that the spectrum of OCT  
366 geometries is wide and passive margin morphologies often differs from these “magma-rich” /  
367 “magma-poor” end-member archetypes (Fig. 1, e.g., **Fernandez et al., Nirrengarten et al.,**  
368 this issue). The distal margin of one of these examples, the South China Sea, has recently  
369 been drilled by IODP expeditions 367-368-368X (Larsen et al., 2018; Ding et al., 2019;  
370 **Nirrengarten et al.,** this issue) bringing new data that challenges our understanding of  
371 continental breakup processes. Rifting style in the South China Sea was primarily controlled  
372 by the presence of a weak lower crust (Franke et al., 2014; Brune et al., 2014; 2017) and its  
373 ability to flow during rifting (**Bai et al.,** this issue). Thinning of the continental crust in the  
374 areas drilled by the IODP Consortium occurs in a series of rift basins largely controlled by  
375 listric faults (**Zhang et al.** this issue), which sole out at different crustal levels (e.g., Liang et  
376 al., 2019; Ding et al., 2019; **Nirrengarten et al.,** this issue). IODP drilling results combined  
377 with high-resolution seismic and potential field data confirmed the narrowness of the OCT in  
378 this same region (Pichot et al., 2014; Cameselle et al., 2017) and revealed that is made of thin  
379 continental crust with shallow extrusive rocks and deep intrusions (Larsen et al., 2018; Ding  
380 et al., 2019; **Nirrengarten et al.,** this issue). The OCT structure was interpreted as resulting  
381 from rapid continental breakup (Larsen et al., 2018; Ding et al., 2019). Going a step further,

382 the assessment made by **Nirrengarten et al.**, (this issue) concerning the amount of tectonic  
383 extension vs. magmatic accretion at the OCT and oceanic crust, for the same region of the  
384 South China Sea drilled by IODP, showed that continental breakup was followed by an initial  
385 transient phase of asymmetric spreading. This highlights the complex interplay between  
386 tectonic and magmatic processes during and after continental breakup.

387 The different case studies presented in this issue confirm that the timing, volume and  
388 location of magmatism are highly variable in OCT reflecting different initial geodynamic  
389 settings. A number of competing parameters may influence the magmatic production such as  
390 extension rates, the initial lithosphere geotherm, crustal rheology and initial crustal thickness  
391 (Davis and Lavier, 2017). In addition to considerations on the magmatic production, which  
392 remains difficult to quantify precisely (Peron-Pinvidic et al., 2016), it is also fundamental to  
393 investigate the relative importance between tectonic and magmatic processes to apprehend  
394 the diversity of continental breakup mechanisms (Tugend et al., 2020). Additional insights  
395 come from the analysis of stratigraphic sequences deposited during continental breakup  
396 (“breakup sequences” Soares et al., 2012; Lei et al., 2019). These breakup sequences  
397 represent a unique record of the depositional environments and subsidence history during and  
398 after continental breakup, representing key questions to address the thermal evolution of  
399 passive margins and generation of potential petroleum systems (Alves et al., 2020).

400

#### 401 **4. Evaporite distribution, salt tectonics and fluid migration on continental margins**

402 Salt basins often form an integral part of the evolution of continental margins. Due to  
403 their fast depositional rate, they can create giant salt bodies (100s of meters to few kilometres  
404 thick), which are very prominent in the stratigraphic record (Warren, 2016). Furthermore, the

405 distinctive acoustic response of evaporites, makes them excellent stratigraphic markers on  
406 seismic reflection data, and thus, clear geodynamic indicators in continental margins  
407 evolution. The presence of thick salt modifies the geothermal gradient of the basin due to the  
408 high conductivity of this mineral (e.g., Petersen and Lerche 1995). It also produces a unique  
409 structural style, with the development of salt tectonics and the creation of multiple, often  
410 deep, detachment levels (e.g. Jackson and Hudec, 2017). Additionally, the nearly  
411 impermeable nature of buried salt modifies the behaviour of subsurface fluid migration and  
412 acts as a seal to subjacent ascending fluids, such as hydrocarbons (e.g. Gluyas and Swarbrick,  
413 2009).

414         While the composition of evaporitic basins is highly variable, halite (rock salt)  
415 dominates the deposits of salt giants associated to continental margins. This mineral has a  
416 thermal conductivity two to four times greater than that of other sedimentary rocks found in  
417 oil- and gas-bearing basins (Petersen and Lerche, 1995; Mello et al. 1995; Magri et al. 2008).  
418 The temperature distribution through time in the subsurface of a basin hosting a salt giant has  
419 an impact on the generation of hydrocarbons, which is delayed (Zhuo et al., 2016) and on  
420 geothermal energy (Grey and Nunn, 2010). **Hassan et al.** (this volume) note how some  
421 continental margins can show a two-phase response to salt deposition: short-term thermal  
422 equilibration between the salt and crust and longer-term relaxation in which the salt basin  
423 thermal image penetrates to a depth about its width (Goteti et al 2013).

424         This special volume includes contributions from amongst the largest salt giants on  
425 continental margins, located in the Barents Sea, North Atlantic, Gulf of Mexico, and South  
426 Atlantic salt provinces (Fig. 2). While the tectonic development of giant salt basins has been  
427 largely studied, comparatively little attention has been given to the paleogeographic and

428 geodynamic conditions that allow the deposition of thick and spatially widespread evaporites  
429 in the early stages of development of continental margins. This includes the large-scale  
430 factors that control the mineralogical composition, thickness and distribution of salt giants on  
431 continental margins. The conditions of restricted deep evaporitic basin are usually associated  
432 with a fast depositional rate and considerable thickness of evaporites, such as 3-4 km of salt  
433 in 2 Ma, in the Gulf of Mexico (**Roelofse et al.** this volume), not dissimilar to the rates  
434 observed in the Mediterranean Messinian (Ryan et al., 2009) and in the Brazil South Atlantic  
435 salt (**Szatmari et al.** this volume, Pietzsch et al., 2018). The variety of examples presented in  
436 this volume allows comparing and contrasting the different structural and paleogeographic  
437 controls on evaporite deposition and show how the identification of sub-salt depocentres and  
438 syn-rift structures, hindered by the challenges of sub-salt imaging (see e.g. **Fernandez et al.**,  
439 this volume), can be aided by interpretation of the thickness variations, and evaporite facies  
440 (**Hassan et al.**, this volume).

441 **Hassan et al.** (this volume) show how the Pennsylvanian to early Permian evaporites  
442 of the southeastern Norwegian Barents Sea contain a thick sequence of mobile halite, while  
443 on the structural highs anhydrite (non-mobile) is the dominant lithology. In the Aquitaine  
444 Basin region (France), thick bodies of evaporites (up to 1000 m thick) accumulated in sub-  
445 basins formed by the initiation (or reactivation) of major north-dipping normal faults, linked  
446 to incipient rifting between the modern-day Europe and Iberia plates during the latest Triassic  
447 and earliest Jurassic (**Benoit et al.**, this volume). **Roelofse et al.** (this volume) summarise how  
448 in the Gulf of Mexico, the middle Jurassic Louann salt was deposited in a relatively deep, a  
449 semi-restricted basin originally formed in the Late Triassic by the rift of the North American  
450 plate from Pangaea, and followed by an Early Jurassic transgression. Early Mesozoic basins

451 in West Iberia, Newfoundland, and the North Sea show a tripartite depositional evolution of  
452 stacked continental, evaporitic, and marine strata suggesting a co-genetic evolution of these  
453 basins along the North Atlantic margin, favouring the interpretation that a seaway existed  
454 during the early stages of continental rifting spanning from the Lusitanian to the Peniche and  
455 Porto Basins. (**Walker et al.**, this volume). Therefore, mapping the distribution of the salt  
456 sheds light on the geometry and subsidence history of early rift basins in a segment of the  
457 North Atlantic (**Walker et al.**, this volume). **Fernandez et al.** (this volume) show that  
458 volcanism synchronous with the late stages of passive margin development, and related  
459 hydrothermalism, can account for the high alkalinity that dominated the pre-salt lacustrine  
460 environments and could also have contributed to the modification of marine waters that led to  
461 the deposition of the thick Aptian evaporites in the South Atlantic Ocean. In West Africa.  
462 The evaporite unit is generally considered to be the last unit deposited prior to lithospheric  
463 breakup and oceanic crust formation between Africa and South America. The evaporite unit  
464 is therefore used to separate stratigraphy into pre- or sub-salt units below and post-salt units  
465 above, that equate to talking of pre- and post-oceanic (pre- and post-breakup) sediments  
466 (**Fernandez et al.**, this volume).

467 Many of the world's prolific hydrocarbon reservoirs are associated with traps created  
468 by salt structures that develop in salt tectonics-deformed basins (as summarised in Warren,  
469 2017, Jackson and Hudec, 2017) (Fig. 2). The presence of thick evaporitic salt within rifted  
470 continental margins has a profound and unique influence on the evolution of the overlying  
471 sedimentary sequences (Hudec and Jackson, 2007) and is seen in examples such as the Gulf  
472 of Mexico, South Atlantic American and African margins, Scotian basin, North Sea and other  
473 European basins (e.g., Diegel et al., 1995; Davison, 2007; Hudec and Jackson, 2007; Gaullier

474 and Vandeville, 2005; Rowan et al, 2012; Goteti et al., 2013) Salt is mechanically weak layer  
475 in comparison to the surrounding lithologies and can flow over the time span of the basin  
476 evolution at particular (> 500 m) burial depths (Jackson and Hudec, 2017, and references  
477 therein). While an extensive literature exists on salt tectonics mechanics, triggers and  
478 geometry, the studies contained in this volume address specifically the influence of evaporite  
479 composition and distribution on the salt tectonics signal of the basin, and the effect of pre-salt  
480 structure in the later development of salt tectonics, which have been comparatively less  
481 addressed.

482         In salt giants, the deformation style of the evaporites depends on their composition.  
483 **Hassan et al.** (this volume) describe how the lithological contrast of mobile and non-mobile  
484 evaporites bodies had an effect on halokinesis in the Barent Sea. Here, the Carboniferous  
485 structures controlled the volume, thickness and lithological alterations of the evaporites, and  
486 have later influenced the distribution and development of the salt wall and domes. The  
487 evolution of salt walls and domes was poly-phased recording the structural development of  
488 the basin, and the changes in plate tectonics motions. Conversely, in the west Iberia salt  
489 basins, halokinesis in the depocentres was related to regional extension and half-graben  
490 collapse, a style of salt tectonics which is common in active rift basins, and on the outer shelf  
491 and upper slope of passive margins (Hudec and Jackson, 2007). Where precursor diapirs are  
492 absent, thickness of the evaporite deposit is the main control on structural style. Above thick  
493 salt, diapirs and adjacent withdrawal basins grow larger (**Walker et al.**, this volume). **Benoit**  
494 **et al** (this volume) highlight how pre-rift Triassic salt in the décollements is able to separate  
495 the structural styles of sub- and supra-salt successions, within the development of the  
496 Aquitaine Basin of the Pyrenean rift system. In this basin, the link of salt tectonic to local and

497 larger scale basin development is twofold: salt diapirs controlled local synclines, and were  
498 emplaced above basement faults. Accommodation in the nearby Arzacq Basin was instead  
499 controlled by salt tectonic induced by extensional strain localisation on inherited structures,  
500 including large-scale salt diapirism and salt-detachment synclines.

501         The presence of a large halite-dominated evaporitic body has a large influence on the  
502 distribution of pore fluids and pressures. In particular, halite possess excellent intrinsic  
503 sealing properties (Downey, 1984; Gluyas and Swarbrick, 2009; Hunt, 1990). Uncompacted  
504 salt crystals can have the same permeability as an unconsolidated clastic deposit with an  
505 equivalent hydraulic grain radius. However, after a few 100s m of burial the permeability  
506 may be reduced to the order of nD or  $10^{-21}$  m<sup>2</sup> (Ingebritsen et al., 2006). Therefore, halite  
507 dominated evaporites can act as a barrier to subjacent upwelling fluids, and potentially  
508 generate overpressure in the sediments underlying the evaporites. This rapid drop in  
509 permeability to the nano-Darcy range has led to the traditional view of salt giants as  
510 representing effectively impermeable barriers to fluid flow (Downey, 1984; Gluyas and  
511 Swarbrick, 2009; Warren, 2017). The rapid sedimentation rates of halite can quickly form a  
512 tight seal and retard or inhibit compaction-led dewatering, leading to overpressure build-up:  
513 many of the world's largest oil and gas fields are sealed by evaporites (Warren, 2017).

514         Once the basin is deformed by salt tectonics, fluid migration and leakage from pre- to  
515 post-evaporite series is driven by pathways along diapirs, salt walls, and across welds, as  
516 described for the Gulf of Mexico by **Roelofse et al** (this volume). Intrusive magmatic bodies  
517 and hydrothermal activity also are factors contributing to salt breach (Schofield et al., 2014).  
518 However, bypass of undeformed thick evaporites is also possible (Warren, 2017). As  
519 overpressure builds-up up to hydrofracturing even during the deposition of halite and the

520 significant sea-level fluctuations occurring in a giant evaporite basin, this may result in fluid  
521 expulsion at different stages of its development (Kukla et al., 2011; Bertoni and Cartwright  
522 2015; Cartwright et al., 2021; Dale et al., 2021). This process has been documented by the  
523 evidence of cross-salt fluid migration pathways, observed on seismic data (Davison, 2009;  
524 Bertoni et al., 2017; Cartwright et al. 2018; Kirkham et al 2020). Additional factors that  
525 control leakage in undeformed salt are lithological heterogeneities within the evaporites  
526 (Anderson and Kirkland, 1980; Schoenherr et al., 2007), dissolution (Anderson and Kirkland,  
527 1980; Kastens and Spiess, 1984) and deep burial (Ghanbarzadeh et al., 2015). The  
528 exceptional situations where leakage happens across salt units are important to recognise not  
529 only for understanding seal risk in hydrocarbon exploration, but also for underground storage  
530 of waste or gas (Warren, 2017). Even in continental margins with no evaporites, an  
531 exceptionally active fluid flow system can be prominent and help identify deep structure and  
532 active faulting. Micallef et al (this volume) show through the interpretation of gas migration  
533 and seepage that the onshore and faults systems offshore the Maltese Islands in the Eastern  
534 Mediterranean, are permeable and that they were active recently and simultaneously. The  
535 latter can be explained by a transtensional system involving two right-stepping, right-lateral  
536 NW-SE trending faults. Such a configuration may be responsible for the generation or  
537 reactivation of faults and fits into the modern divergent strain-stress regime inferred from  
538 geodetic data.

539

## 540 **5. Post-rift evolution of continental margins**

541 The term ‘passive margin’ originated from the belief that rifted continental margins  
542 experienced little deformation following plate separation (e.g. Bond and Kominz, 1988). In

543 recent years however, a large body of evidence has accumulated for post-rift compressional  
544 deformation of sedimentary successions at several margins around the world including Brazil  
545 (**Bezzera et al., 2020**, this issue), West Africa (Hudec and Jackson, 2002), and NW Australia  
546 (Hillis et al., 2008). A characteristic feature of post-breakup deformation is the formation of  
547 commonly dome-shaped growth anticlines that represent attractive petroleum exploration  
548 targets (Lundin and Doré, 2002). Many of these structures are fault-propagation folds that  
549 grew above reverse-reactivated syn-rift faults, although some appear to be unrelated to fault  
550 reactivation (Doré et al., 2008). Localised compressional shortening at passive margins is  
551 often superimposed on regional uplift that is manifested by long-wavelength (>200-500 km)  
552 low-angle ( $\leq 5^\circ$ ) unconformities (Doré et al., 2002; Praeg et al., 2005; Johnson et al., 2008).  
553 Given that post-breakup sedimentary sequences accumulate near-continuously at sediment-  
554 nourished rifted margins in response to their thermally-controlled subsidence, the resulting  
555 stratigraphic successions can allow precise dating of post-breakup structures, which can in  
556 turn provide unique insights into the roles and temporal variability of extrinsic tectonic  
557 forcing and intrinsic mechanical properties of continental lithosphere in controlling  
558 deformation in intraplate environments.

559         Despite increasing recognition of post-breakup compressional deformation at rifted  
560 margins, there is little consensus regarding the principal extrinsic tectonic driving forces. To  
561 date, tectonic models for post-breakup deformation include: transmission of stresses from  
562 collisional plate boundaries (Ziegler et al., 1995); body forces resulting from mid-ocean  
563 ridges (Doré et al., 2008) or uplifted margin topography (Pascal and Cloetingh, 2009); shear  
564 traction at the base of the lithosphere which may be enhanced by asymmetric seafloor  
565 spreading (Mosar et al., 2002); and reactivation of basement lineaments (Doré and Lundin,

1996). Understanding the chronology of post-breakup compressional deformation at passive margins is essential if the principal extrinsic driving mechanisms are to be determined (Doré et al., 2008). Many studies have noted episodicity when describing post-breakup deformation, with phases of reactivation along localized fault systems and resultant fold growth occurring within discrete time intervals, commonly of no more than several Myr (Boldreel and Anderson, 1998; Doré et al., 2008). In this section, we review the chronologies of deformation at two rifted margins that witness spatially and temporally extensive post-breakup deformation; the southern Australian and NW European margins. Our analysis indicates that although enhanced increments of deformation along localized fault systems take place within discrete time intervals, the margin-wide response to compressional forcing at these margins has occurred near-continuously post-breakup.

The southern Australian margin formed following Cretaceous-Paleogene rifting between Australia and Antarctica (Norvick and Smith, 2001; Holford et al., 2011). Breakup propagated eastwards, with seafloor spreading initiated south of the Bight Basin during the late Albian-early Campanian (~95-83 Ma), and final breakup south of the Otway at ~43 Ma (intra-Lutetian) coinciding with the onset of fast spreading in the Southern Ocean (Norvick and Smith, 2001). Eastern parts of the margin were also influenced by opening of the Tasman Sea, which ceased at ~52 Ma (Norvick and Smith, 2001). These rifting events resulted in a number of major Cretaceous-Cenozoic depocentres that contain up to several kilometres of post-breakup siliciclastic and calcareous sediments, including the Otway and Gippsland basins. Previous studies have identified a major compression episode along southeastern parts of the margin during the late Miocene-early Pliocene, marked by a regional tectonic unconformity (~10-5 Ma) (Dickinson et al., 2002). We find that the late Miocene-early

589 Pliocene compression phase is characterised by growth of ~NE-SW to ENE-WSW trending  
590 folds, often situated above reverse-reactivated normal fault systems and is primarily evident  
591 in the eastern Otway Basin and the Torquay-sub-basin adjacent to the Otway Ranges  
592 (Holford et al., 2014), which were uplifted at this time (Sandiford et al., 2004), and in the  
593 Gippsland Basin (Dickinson et al., 2001; Mahon and Wallace, 2020) (Fig. 3). Offshore  
594 seismic data and onshore geomorphological and stratigraphic observations indicate that  
595 growth of some folds has continued throughout the Pliocene and in some cases into the  
596 Pleistocene e.g. Ferguson Hill Anticline, Otway Basin (until ~2-1 Ma; Sandiford, 2003).  
597 Earlier deformation is observed in the western Otway Basin, where seismic mapping of a  
598 regional intra-Lutetian-age unconformity reveals that large folds such as the Morum and  
599 Copa anticlines formed during the mid-Eocene (Holford et al., 2014; Fig. 3). The latter  
600 structure also reveals evidence for late Oligocene-early Miocene growth (Fig. 3), whilst the  
601 Argonaut and Minerva anticlines witness growth during the early-mid Miocene (Holford et  
602 al., 2014). In the Gippsland Basin, seismic mapping reveals an onset of widespread  
603 compressional tectonism at the Eocene-Oligocene boundary (~34 Ma), with major growth on  
604 compressional structures such as the Barracouta and Dolphin anticlines continuing until the  
605 early Miocene (~20 Ma; Mahon and Wallace, 2020).

606         The NW European margin formed following multiple Permian-Paleogene rifting  
607 episodes, with continental breakup between NW Europe and Greenland achieved by ~53.7  
608 Ma (Doré et al., 2008). The post-breakup sedimentary record of the margin is dominated by  
609 multiple, Eocene and younger, siliclastic sediment wedges that prograde from the continental  
610 shelves of the British Isles, Norway and Faroe Islands, accompanied by the deposition of  
611 deep-water contourites in the adjacent basins since late Eocene time (Stoker et al., 2010).

612 Previous studies have documented widespread compressional folding on the Rockall-Faroes-  
613 West Shetland and mid-Norwegian sections of this margin, with particularly intense phases  
614 of deformation identified during the mid-Eocene to Oligocene and early-mid Miocene  
615 (Boldreel and Anderson, 1998; Lundin and Doré, 2002; Stoker et al., 2005).

616 Our compilation of timing estimates for post-breakup compressional structures on the  
617 NW European margin is primarily based on seismic mapping by the British Geological  
618 Survey in the Rockall-Faroes-West Shetland area (Stoker et al., 2005; Ritchie et al., 2008)  
619 and by multiple mapping studies of structures located on the mid-Norwegian margin (Fig. 4).  
620 Major structures located in the Vøring Basin on the mid-Norwegian margin generally trend  
621 ~NE-SW to N-S (Fig. 4) and include the Ormen Lange Dome and Helland-Hansen Arch, the  
622 latter of which has an amplitude of ~1 km and axial trace length of ~200 km (Doré et al.,  
623 2008). Both these structures have documented mid-Eocene-early Oligocene growth phases  
624 and were reactivated during the early-mid Miocene when folds including the Vema and  
625 Hedda domes also developed (Lundin and Doré, 2002). As described by Omosanya (2020) in  
626 this special issue, the Naglfar Dome witnesses multiphase post-breakup growth, with tectonic  
627 inversion commencing in the early Eocene to Oligocene, and subsequent inversion during the  
628 early Miocene. Post-breakup structures in the Rockall-Faroes-West Shetland area exhibit a  
629 wide variation in scale (axial trace lengths <10 to >250 km), orientation and timing (Fig. 4),  
630 and some may record a component of transpressional deformation (Ritchie et al., 2008). The  
631 largest structures include the Fugloy, Munkagrannur and Wyville Thomson ridges (Fig. 4),  
632 which form prominent bathymetric highs with reliefs of  $\leq 900$  m (Stoker et al., 2005). Seismic  
633 mapping reveals significant early-mid Miocene growth of these structures (Stoker et al.,  
634 2005), but also reveals long-lived growth of the latter throughout the Eocene-Oligocene

635 (Ritchie et al., 2008). Other structures with long-lived growth histories include the North  
636 Hatton Bank Fold Complex on the Hatton High (mid-Eocene to early Oligocene). In the NE  
637 Faeroe-Shetland Basin there are numerous NE-SW and NNE-SSE trending growth folds that  
638 developed in the early-mid Miocene and early Pliocene, and some of the younger structures  
639 have associated raised seabed profiles suggesting ongoing compression (Ritchie et al., 2008).

640 The compiled data on the timing of post-breakup compressional deformation at the  
641 southern Australian and NW European passive margins exhibit some similarities, with clear  
642 ‘peaks’ of enhanced compressional activity (e.g. early-mid Miocene in NW Europe, late  
643 Miocene-early Pliocene in southern Australia), but also evidence for fold growth over  
644 extended periods following breakup, defining a near-continuous history of deformation.

645 The majority of post-breakup folds in the southern Australian margin trend ~NE-SW in  
646 the Otway Basin with a slight rotation to ~ENE-WSW in the Gippsland Basin (Fig. 4). The  
647 orientations of paleostresses inferred from these structures are highly consistent with  
648 independent determinations of the present-day stress field, which indicate ~NW-SE-oriented  
649 maximum horizontal stress ( $\sigma_{Hmax}$ ) that rotates to ~E-W along eastern parts of the margin  
650 (Reynolds et al., 2002; Sandiford et al., 2004; Tassone et al., 2017). Post-breakup structures  
651 on the NW European margin exhibit larger variation in orientation, particularly in the Rockall  
652 area (Fig. 4). This variation at least partially reflects the protracted and complex rifting  
653 history of this margin (Doré et al., 1999), and the influence of syn-breakup magmatism  
654 (Schofield et al., 2017; Omosanya, 2020). Fold trends show more consistency in the Faeroe-  
655 Shetland Basin (mostly ~NE-SW) and offshore Norway (broadly ~N-S) (Fig. Y). Paleostress  
656 orientations from these structures are again largely consistent with observed ~NW-SE  
657 present-day  $\sigma_{Hmax}$  (Holford et al., 2016). Finite element models applied to the Indo-

658 Australian (Reynolds et al., 2002) and NW European plates (Gölke and Coblenz, 1996) show  
659 that the mild compressional stress regimes at both margins are consistent with first-order  
660 control by the balance between collisional torques along plate boundary segments that resist  
661 plate motion, and the plate driving torques associated with cooling oceanic lithosphere (ridge-  
662 push) and subduction (slab-pull) (Sandiford et al., 2004). Given that the majority of post-  
663 breakup structures at both margins exhibit broadly similar trends (irrespective of their ages)  
664 that are consistent with both observed and modelled present-day  $\sigma_{Hmax}$ , we propose that  
665 their origin is likely related to extrinsic forcing controlled by plate boundary configurations.  
666 The continuous aspect of post-breakup deformation we report is consistent with the notion  
667 that intraplate stress systems are continuously renewed by plate boundary stress sources such  
668 as ridge-push and slab-pull (Bott and Kusznir, 1984), resulting in constant or steadily  
669 changing extrinsic forcing that is coupled to plate boundary evolution. At both margins,  
670 observed periods of widespread, higher strain-rate deformation coincide closely with  
671 important plate boundary reconfigurations (Figs. 3, 4). These correlations may reflect either  
672 (i) increased forcing, or (ii) intrinsic responses of passive margin fault systems to changing  
673 stress fields. Examples of episodic deformation caused by increased forcing may have  
674 occurred in the late Miocene-early Pliocene along the southern Australian margin, and the  
675 mid-Miocene along the NW European margin. Sandiford et al. (2004) show that the late  
676 Miocene-early Pliocene peak in tectonic activity in the Otway and Gippsland basins can be  
677 explained by increased coupling of the Australian and Pacific plate boundary that may have  
678 increased stress magnitudes to levels sufficient to initiate slip on previously dormant fault  
679 sets. Doré et al. (2008) suggest that the mid-Miocene acme of deformation along the NW  
680 European margin can be explained by enhanced body forces, and thus intraplate stress  
681 magnitudes, resulting from development of the Iceland insular margin on the North Atlantic

682 ridge-system during the middle Miocene. This enhanced ridge-push forcing, combined with  
683 the presence of hyperextended and weakened lithosphere (Lundin and Doré, 2011), may  
684 account for the larger dimensions of post-breakup structures on the NW European margin.

685       Episodic increments of enhanced post-breakup deformation might also, at least  
686 partially, represent intrinsic mechanical responses of intraplate fault systems to changing  
687 stress states. Finite element models such as those applied to the NW European and Indo-  
688 Australian plates (Gölke and Coblenz, 1996; Reynolds et al., 2002) show that intraplate  
689 stress orientations are highly sensitive to both the forces that act along plate boundaries and  
690 the disposition of these boundaries. Consequently, significant plate boundary  
691 reconfigurations are likely to result in changing intraplate stress orientations, which may  
692 rejuvenate slip along many faults that were previously unfavourably oriented for reactivation.  
693 An additional possibility is that changes in stress magnitude or state are accompanied by  
694 widespread fluid overpressure generation, which facilitates reactivation of steeply dipping  
695 rift-related normal faults (Sibson, 1995).

696

## 697 **References**

698 Alves, T. M., and Cunha, T. A. 2018. A phase of transient subsidence, sediment bypass and  
699 deposition of regressive–transgressive cycles during the breakup of Iberia and  
700 Newfoundland. *Earth and Planetary Science Letters*, 484, 168-183.

701 Alves, T., Fetter, M., Busby, C., Gontijo, R., Cunha, T. A., and Mattos, N. H. 2020. A  
702 tectono-stratigraphic review of continental breakup on intraplate continental margins and its  
703 impact on resultant hydrocarbon systems. *Marine and Petroleum Geology*, 117, 104341.

704 Anderson, R.Y., Kirkland, D.W., 1980. Dissolution of salt deposits by brine density flow.  
705 *Geology* 8, 66-69.

706 Bertoni, C. and Cartwright, J., 2015. Messinian evaporites and fluid flow. *Marine and*  
707 *Petroleum Geology*, 66, 165-176.

708 Bertoni, C., Kirkham, C., Cartwright, J., Hodgson, N., Rodriguez, K., 2017. Seismic  
709 indicators of focused fluid flow and cross-evaporitic seepage in the Eastern Mediterranean.  
710 *Marine and Petroleum Geology*, 88, 472-488.

711 Bezerra, F.H., de Castro, D.L., Maia, R.P., Sousa, M.O.L., Moura-Lima, E.N., Rossetti, D.F.,  
712 Bertotti, G., Souza, Z.S., and Nogueira, F.C.C., 2020, Postrift stress field inversion in the  
713 Potiguar Basin, Brazil – Implications for petroleum systems and evolution of the equatorial  
714 margin of South America: *Marine and Petroleum Geology*, v. 111, 88-104.

715 Boldreel, L.O, and Anderson, M.S., 1998, Tertiary compressional structures on the Faeroe-  
716 Rockall Plateau in relation to northeast Atlantic ridge-push and Alpine foreland stresses:  
717 *Tectonophysics*, v. 300, 13-28.

718 Bond, G.C., and Kominz, M.A., 1988, Evolution of thought on passive continental margins  
719 from the origin of geosynclinal theory (~1860) to the present: *Geological Society of America*  
720 *Bulletin*, v. 100, 1903-1933.

721 Bott, M.H.P. and Kusznir, N.J., 1984, The origin of tectonic stress in the lithosphere:  
722 *Tectonophysics*, v. 105, 1-13.

723 Brune, S., Heine, C., Pérez-Gussinyé, M., and Sobolev, S. V. (2014). Rift migration explains  
724 continental margin asymmetry and crustal hyper-extension. *Nature communications*, 5(1), 1-  
725 9.

726 Brune, S., Heine, C., Clift, P. D., and Pérez-Gussinyé, M. (2017). Rifted margin architecture  
727 and crustal rheology: reviewing Iberia-Newfoundland, central South Atlantic, and South  
728 China Sea. *Marine and Petroleum Geology*, 79, 257-281.

729 Buck, W. R. 2004, "1. Consequences of Asthenospheric Variability on Continental Rifting".  
730 *Rheology and Deformation of the Lithosphere at Continental Margins*, edited by Garry D.  
731 Karner, Brian Taylor, Neal W. Driscoll and David L. Kohlstedt, New York Chichester, West  
732 Sussex: Columbia University Press, pp. 1-30. <https://doi.org/10.7312/karn12738-002>

733 Buck, W. R. (2017). The role of magmatic loads and rift jumps in generating seaward dipping  
734 reflectors on volcanic rifted margins. *Earth and Planetary Science Letters*, 466, 62-69.

735 Cameselle, A. L., Ranero, C. R., Franke, D., and Barckhausen, U. (2017). The continent-  
736 ocean transition on the northwestern South China Sea. *Basin Research*, 29, 73-95.

737 Cartwright, J., Kirkham, C., Foschi, M., Hodgson, N., Rodriguez, K. and James, D., 2021.  
738 Quantitative reconstruction of pore-pressure history in sedimentary basins using fluid escape  
739 pipes. *Geology*, in press.

740 Chauvet, F., Sapin, F., Geoffroy, L., Ringenbach, J. C., and Ferry, J. N. (2020). Conjugate  
741 volcanic passive margins in the austral segment of the South Atlantic—Architecture and  
742 development. *Earth-Science Reviews*, 103461.

743 Clerc, C., Jolivet, L., and Ringenbach, J. C. (2015). Ductile extensional shear zones in the  
744 lower crust of a passive margin. *Earth and Planetary Science Letters*, 431, 1-7.

745 Clerc, C., Ringenbach, J. C., Jolivet, L., and Ballard, J. F. (2018). Rifted margins: Ductile  
746 deformation, boudinage, continentward-dipping normal faults and the role of the weak lower  
747 crust. *Gondwana Research*, 53, 20-40.

748 Coffin, M. F., and Eldholm, O. (1994). Large igneous provinces: crustal structure,  
749 dimensions, and external consequences. *Reviews of Geophysics*, 32(1), 1-36.

750 Dale, M. S., Marín-Moreno, H., Falcon-Suarez, I. H., Grattoni, C., Bull, J.M., McNeill, L.C.,  
751 2021. The Messinian Salinity Crisis as a trigger for high pore pressure development in the  
752 Western Mediterranean. *Basin Research*, in press.

753 Davis, M., and Kusznir, N. (2004). 4. Depth-Dependent Lithospheric Stretching at Rifted  
754 Continental Margins. In *Rheology and deformation of the lithosphere at continental margins*  
755 (pp. 92-137). Columbia University Press.

756 Davis, J. K., and Lavier, L. L. (2017). Influences on the development of volcanic and  
757 magma-poor morphologies during passive continental rifting. *Geosphere*, 13(5), 1524-1540.

758 Davison, I., 2007, Tectonics of the Brazilian Atlantic margin salt basins, in *Deformation of*  
759 *the Continental Crust: The Legacy of Mike Coward*, edited by A. Reis, R. W. H. Butler, and  
760 R. H. Graham, Geological Society of London Special Publication, 272, 345–359.

761 Davison, I., 2009. Faulting and fluid flow through salt. *J. Geol. Soc.* 166, 205-216.

762 Debenham, N., King, R.C. and Holford, S.P., 2018, The influence of a reverse-reactivated  
763 normal fault on natural fracture geometries and relative chronologies at Castle Cove, Otway  
764 Basin: *Journal of Structural Geology*, v. 112, 112-130.

765 Debenham, N., Farrell, N.J., Holford, S.P., King, R.C. and Healy, D., 2019, Spatial  
766 distribution of micrometre-scale porosity and permeability across the damage zone of a  
767 reverse-reactivated normal fault in a tight sandstone: Insights from the Otway Basin, SE  
768 Australia: *Basin Research*, v. 31, 640-658.

769 Desmurs, L., Müntener, O., and Manatschal, G. (2002). Onset of magmatic accretion within a  
770 magma-poor rifted margin: a case study from the Platta ocean-continent transition, eastern  
771 Switzerland. *Contributions to Mineralogy and Petrology*, 144(3), 365-382.

772 Dickinson, J.A., Wallace, M.W., Holdgate, G.R., Daniels, J., Gallagher, S.J., and Thomas, L.,  
773 2001, Neogene tectonics in SE Australia: implications for petroleum systems: *APPEA*  
774 *Journal*, v. 41, 37-52.

775 Diegel, F. A., J. F. Karlo, D. C. Schuster, R. C. Shoup, and P. R. Tauvers, 1995. Cenozoic  
776 structural evolution and tectono-stratigraphic framework of the northern Gulf Coast  
777 continental margin, in *Salt Tectonics, a Global Perspective*, edited by M. P. A. Jackson, D.  
778 G. Roberts, and S. Snelson, *AAPG Memoir*, 65, 109–151, American Association of  
779 Petroleum Geologists, Tulsa, Okla.

780 Ding, W., Sun, Z., Mohn, G., Nirrengarten, M., Tugend, J., Manatschal, G., and Li, J. (2020).  
781 Lateral evolution of the rift-to-drift transition in the South China Sea: Evidence from multi-  
782 channel seismic data and IODP Expeditions 367 and 368 drilling results. *Earth and Planetary*  
783 *Science Letters*, 531, 115932.

784 Doré, A.G., and Lundin, E.R., 1996, Cenozoic compressional structures on the NE Atlantic  
785 margin: nature, origin and potential significance for hydrocarbon exploration: *Petroleum*  
786 *Geoscience*, v. 2, 299-311.

787 Doré, T., and Lundin, E. (2015). Research focus: Hyperextended continental margins—  
788 knowns and unknowns. *Geology*, 43(1), 95-96.

789 Doré, A.G., Lundin, E.R., Kusznir, N.J. and Pascal, C., 2008, Potential mechanisms for the  
790 genesis of Cenozoic domal structures on the NE Atlantic margin: pros, cons, and some new

791 ideas, in Johnson, H., et al., eds., The nature and origin of compression in passive margins:  
792 Geological Society of London Special Publication 306, 1-26.

793 Downey, M.W., 1984. Evaluating seals for hydrocarbon accumulations. AAPG Bull. 68,  
794 1752-1763.

795 Duncan, R.A., Larsen, H.C., and Allan, J.F. (eds). 1996. Proceedings of the Ocean Drilling  
796 Program. Initial Reports, 163. Ocean Drilling Program, Texas AandM University, College  
797 Station, TX, <https://doi.org/10.2973/odp.proc.ir.163.1996>

798 Eldholm, O., Thiede, J. and Taylor, E. (eds). 1987. Proceedings of the Ocean Drilling  
799 Program. Initial Reports, 104. Ocean Drilling Program, Texas AandM University, College  
800 Station, TX, <https://doi.org/10.2973/odp.proc.ir.104.1987>

801 Eldholm, O., Thiede, J. and Taylor, E. 1989. Evolution of the vøring volcanic margin. In:  
802 Proceedings of the Ocean Drilling Program. Scientific Results, 104. Ocean Drilling Program,  
803 Texas AandM University, College Station, TX,  
804 <https://doi.org/10.2973/odp.proc.sr.104.191.1989>

805 Falvey, D. A. (1974). The development of continental margins in plate tectonic theory. The  
806 APPEA Journal, 14(1), 95-106.

807 Fletcher, R., Kusznir, N., and Cheadle, M. (2009). Melt initiation and mantle exhumation at  
808 the Iberian rifted margin: Comparison of pure–shear and upwelling-divergent flow models of  
809 continental breakup. *Comptes Rendus Geoscience*, 341(5), 394-405.

810 Franke, D. (2013). Rifting, lithosphere breakup and volcanism: Comparison of magma-poor  
811 and volcanic rifted margins. *Marine and Petroleum geology*, 43, 63-87.

812 Franke, D., Barckhausen, U., Baristead, N., Engels, M., Ladage, S., Lutz, R., ... and Schnabel,  
813 M. (2011). The continent-ocean transition at the southeastern margin of the South China Sea.  
814 *Marine and petroleum Geology*, 28(6), 1187-1204

815 Franke, D., Savva, D., Pubellier, M., Steuer, S., Mouly, B., Auxietre, J. L., ... and Chamot-  
816 Rooke, N. (2014). The final rifting evolution in the South China Sea. *Marine and Petroleum*  
817 *Geology*, 58, 704-720.

818 Gallahue, M., Stein, S., Stein, C. A., Jurdy, D., Barklage, M., and Rooney, T. (2020). A  
819 compilation of igneous rock volumes at volcanic passive continental margins from  
820 interpreted seismic profiles. *Marine and Petroleum Geology*, 104635.

821 Gaullier, V. and Vendeville, B. C., 2005. Salt tectonics driven by sediment progradation: Part  
822 II—Radial spreading of sedimentary lobes prograding above salt. *AAPG bulletin*, 89(8),  
823 1081-1089.

824 Geoffroy, L., Burov, E. B., and Werner, P. (2015). Volcanic passive margins: another way to  
825 break up continents. *Scientific reports*, 5(1), 1-12.

826 Ghanbarzadeh, S., Hesse, M. A., Prodanović, M. and Gardner, J. E., 2015. Deformation-  
827 assisted fluid percolation in rock salt. *Science*, 350(6264), 1069-1072.

828 Gillard, M., Autin, J., Manatschal, G., Sauter, D., Munsch, M., and Schaming, M. (2015).  
829 Tectonomagmatic evolution of the final stages of rifting along the deep conjugate Australian-  
830 Antarctic magma-poor rifted margins: Constraints from seismic observations. *Tectonics*,  
831 34(4), 753-783.

832 Gillard, M., Autin, J., and Manatschal, G. (2016). Fault systems at hyper-extended rifted  
833 margins and embryonic oceanic crust: Structural style, evolution and relation to magma.  
834 *Marine and Petroleum Geology*, 76, 51-67.

835 Gillard, M., Tugend, J., Müntener, O., Manatschal, G., Karner, G. D., Autin, J., and Ulrich,  
836 M. (2019). The role of serpentinitization and magmatism in the formation of decoupling  
837 interfaces at magma-poor rifted margins. *Earth-Science Reviews*, 196, 102882.

838 Gillard, M., Sauter, D., Tugend, J., Tomasi, S., Epin, M. E., and Manatschal, G. (2017). Birth  
839 of an oceanic spreading center at a magma-poor rift system. *Scientific Reports*, 7(1), 1-6.

840 Gölke, M., and Coblenz, D., 1996, Origins of the European regional stress field:  
841 *Tectonophysics*, v. 266, 11-24.

842 Goteti, R., Beaumont, C. and Ings, S.J., 2013. Factors controlling early stage salt tectonics at  
843 rifted continental margins and their thermal consequences. *Journal of Geophysical Research:*  
844 *Solid Earth*, 118(6), 3190-3220.

845 Gray, T. and Nunn, J., 2010. Geothermal Resource Assessment of the Gueydan Salt  
846 Dome and the Adjacent Southeast Gueydan Field, Vermilion Parish, Louisiana. *Gulf*  
847 *Coast Association of Geological Societies Transactions*, 60, 307-323.

848 Guan, H., Geoffroy, L., Gernigon, L., Chauvet, F., Grigne, C., and Werner, P. (2019).  
849 Magmatic ocean-continent transitions. *Marine and Petroleum Geology*, 104, 438-450.

850 Harkin, C., Kusznir, N., Roberts, A., Manatschal, G., and Horn, B. (2020). Origin,  
851 composition and relative timing of seaward dipping reflectors on the Pelotas rifted margin.  
852 *Marine and Petroleum Geology*, 114, 104235.

853 Heezen, B. C. (1960). Geologic Mapping of Submerged Continental Margins. AAPG  
854 Bulletin, 44(7), 1250-1250.

855 Hillis, R.R., Sandiford, M., Reynolds, S.D., and Quigley, M.C. 2008. Present-day stresses,  
856 seismicity and Neogene-to-Recent tectonics of Australia's 'passive' margins: intraplate  
857 deformation controlled by plate boundary forces., in Johnson, H., et al., eds., The nature and  
858 origin of compression in passive margins: Geological Society of London Special Publication  
859 306, 71-90.

860 Hinz, K. 1981. A hypothesis on terrestrial catastrophes: wedges of very thick oceanward  
861 dipping layers beneath passive margins; their origin and paleoenvironment significance.  
862 Geologisches Jahrbuch, E22, 345–363.

863 Holford, S., Hillis, R., Duddy, I., Green, P., Stoker, M., Tuitt, A., Backé, G., Tassone, D. and  
864 MacDonald, J., 2011. Cenozoic post-breakup compressional deformation and exhumation of  
865 the southern Australian margin: The APPEA Journal, v. 51, 613-638.

866 Holford, S.P., Tuitt, A.K., Hillis, R.R., Green, P.F., Stoker, M.S., Duddy, I.R., Sandiford, M.  
867 and Tassone, D.R., 2014. Cenozoic deformation in the Otway Basin, southern Australian  
868 margin: implications for the origin and nature of post-breakup compression at rifted  
869 margins: Basin Research, v. 26, p.10-37.

870 Holford, S.P., Tassone, D.R., Stoker, M.S. and Hillis, R.R., 2016, Contemporary stress  
871 orientations in the Faroe–Shetland region: Journal of the Geological Society, v. 173, p.142-  
872 152.

873 Hudec, M.R., and Jackson, M.P.A., 2002, Structural segmentation, inversion and salt  
874 tectonics on a passive margin: Evolution of the Inner Kwanza Basin, Angola: Geological  
875 Society of America Bulletin, v. 114, 1222-1244.

876 Hudec, M., and M. P. A. Jackson, 2007, Terra infirma: Understanding salt tectonics, Earth  
877 Sci. Rev., 82, 1–28.

878 Hunt, J.M., 1990. Generation and migration of petroleum from abnormally pressured fluid  
879 compartments (1). AAPG Bull. 74, 1-12.

880 Ingebritsen, S., Sanford, W., Neuzil, C., 2006. Groundwater in Geological Processes.  
881 Cambridge Univ. Press., Cambridge, UK, 562 pp.

882 Jagoutz, O., Müntener, O., Manatschal, G., Rubatto, D., Péron-Pinvidic, G., Turrin, B. D.,  
883 and Villa, I. M. (2007). The rift-to-drift transition in the North Atlantic: A stuttering start of  
884 the MORB machine?. *Geology*, 35(12), 1087-1090.

885 Jeannot, L., Kuszniir, N., Mohn, G., Manatschal, G., and Cowie, L. (2016). Constraining  
886 lithosphere deformation modes during continental breakup for the Iberia–Newfoundland  
887 conjugate rifted margins. *Tectonophysics*, 680, 28-49.

888 Jerram, D. A., Sharp, I. R., Torsvik, T. H., Poulsen, R., Watton, T., Freitag, U., ... and  
889 Machado, V. (2019). Volcanic constraints on the unzipping of Africa from South America:  
890 Insights from new geochronological controls along the Angola margin. *Tectonophysics*, 760,  
891 252-266.

892 Johnson, H., Ritchie, J.D., Hitchen, K., McInroy, D.B., and Kimbell, G.S., 2005, Aspects of  
893 the Cenozoic deformational history of the Northeast Faroe-Shetland Basin, Wyville Thomson  
894 Ridge and Hatton Bank areas, in Doré, A.G., and Vining, B.A., eds., *Petroleum Geology:*

895 North-West Europe and Global Perspectives. Proceedings of the 6<sup>th</sup> Petroleum Geology  
896 Conference: Geological Society, London, pp. 993-1008.

897 Keir, D. (2014). Magmatism and deformation during continental breakup. *Astronomy and*  
898 *Geophysics*, 55(5), 5-18.

899 Kirkham, C., Cartwright, J., Bertoni, C., Van Rensbergen, P., 2020. The genesis of a giant  
900 mud canopy by catastrophic failure of a thick evaporite sealing layer. *Geology* 48 (8): 787–  
901 791.

902 Larsen, H.C., and Saunders, A.D. 1998. Tectonism and volcanism at the southeast Greenland  
903 rifted margin: a record of plume impact and later continental rupture. In: Proceedings of the  
904 Ocean Drilling Program. Scientific Results, 152. Ocean Drilling Program, TexasAandM  
905 University, College Station, TX, <https://doi.org/10.2973/odp.proc.sr.152.240.1998>

906 Larsen, H.C., Saunders, A.D., and Clift, P.D. (eds). 1994. Proceedings of the Ocean Drilling  
907 Program. Initial Reports, 152. Ocean Drilling Program, Texas AandM University, College  
908 Station, TX, <https://doi.org/10.2973/odp.proc.ir.152.1994>

909 Larsen, H. C., Mohn, G., Nirrengarten, M., Sun, Z., Stock, J., Jian, Z., ... and Zhong, L.  
910 (2018). Rapid transition from continental breakup to igneous oceanic crust in the South China  
911 Sea. *Nature Geoscience*, 11(10), 782-789.

912 Lei, C., Alves, T. M., Ren, J., Pang, X., Yang, L., and Liu, J. (2019). Depositional  
913 architecture and structural evolution of a region immediately inboard of the locus of  
914 continental breakup (Liwan Sub-basin, South China Sea). *GSA Bulletin*, 131(7-8), 1059-  
915 1074.

916 Liang, Y., Delescluse, M., Qiu, Y., Pubellier, M., Chamot-Rooke, N., Wang, J., ... and  
917 Meresse, F. (2019). Décollements, detachments, and rafts in the extended crust of Dangerous  
918 Ground, South China Sea: The role of inherited contacts. *Tectonics*, 38(6), 1863-1883.

919 Lundin, E.R., and Doré, A.G., 2002, Mid-Cenozoic post-breakup deformation in the 'passive'  
920 margins bordering the Norwegian-Greenland Sea: *Marine and Petroleum Geology*, v. 19, 79-  
921 93.

922 Lundin, E.R., and Doré, A.G., 2011, Hyperextension, serpentinization, and weakening: A  
923 new paradigm for rifted margin compressional deformation: *Geology*, v. 39, 347-350.

924 Lymer, G., Cresswell, D. J., Reston, T. J., Bull, J. M., Sawyer, D. S., Morgan, J. K., ... and  
925 Shillington, D. J. (2019). 3D development of detachment faulting during continental breakup.  
926 *Earth and Planetary Science Letters*, 515, 90-99.

927 Mahon, E.M., and Wallace, M.W., 2020, Cenozoic structural history of the Gippsland Basin:  
928 early Oligocene onset for compressional tectonics in SE Australia: *Marine and Petroleum*  
929 *Geology*, v. 114, 104243.

930 Manatschal, G., and Müntener, O. (2009). A type sequence across an ancient magma-poor  
931 ocean–continent transition: the example of the western Alpine Tethys ophiolites.  
932 *Tectonophysics*, 473(1-2), 4-19.

933 McCarthy, A., Tugend, J., Mohn, G., Candiotti, L., Chelle-Michou, C., Arculus, R. and  
934 Müntener, O. (2020). A case of Ampferer-type subduction and consequences for the Alps and  
935 the Pyrenees. *American Journal of Science*, 320(4), 313-372.

936 McDermott, C., Collier, J. S., Lonergan, L., Fruehn, J., and Bellingham, P. (2019). Seismic  
937 velocity structure of seaward-dipping reflectors on the South American continental margin.  
938 *Earth and Planetary Science Letters*, 521, 14-24.

939 McDermott, C., Lonergan, L., Collier, J. S., McDermott, K. G., and Bellingham, P. (2018).  
940 Characterization of seaward-dipping reflectors along the South American Atlantic margin and  
941 implications for continental breakup. *Tectonics*, 37(9), 3303-3327.

942 McDermott, K., and Reston, T. (2015). To see, or not to see? Rifted margin extension.  
943 *Geology*, 43(11), 967-970.

944 McKenzie, D. (1978). Some remarks on the development of sedimentary basins. *Earth and*  
945 *Planetary science letters*, 40(1), 25-32.

946 Menzies, M. A., Klemperer, S. L., Ebinger, C. J., and Baker, J. (2002). Characteristics of  
947 volcanic rifted margins. *Special Papers-Geological Society of America*, 1-14.

948 Minshull, T. A., Dean, S. M., White, R. S., and Whitmarsh, R. B. (2001). Anomalous melt  
949 production after continental break-up in the southern Iberia Abyssal Plain. *Geological*  
950 *Society, London, Special Publications*, 187(1), 537-550.

951 Monteleone, V., Minshull, T. A., and Marin-Moreno, H. (2019). Spatial and temporal  
952 evolution of rifting and continental breakup in the Eastern Black Sea Basin revealed by long-  
953 offset seismic reflection data. *Tectonics*, 38(8), 2646-2667.

954 Mosar, J., Lewis, G., and Torsvik, T.H., 2002, North Atlantic sea-floor spreading rates:  
955 implications for the Tertiary development of inversion structures of the Norwegian-  
956 Greenland Sea: *Geological Society [London] Journal*, v. 159, p.503-515.

957 Müntener, O., Manatschal, G., Desmurs, L., and Pettke, T. (2010). Plagioclase peridotites in  
958 ocean–continent transitions: refertilized mantle domains generated by melt stagnation in the  
959 shallow mantle lithosphere. *Journal of Petrology*, 51(1-2), 255-294.

960 Mutter, J.C. 1993. Margins declassified. *Nature*, 364, 393–394,  
961 <https://doi.org/10.1038/364393a0>

962 Mutter, J.C., Buck, W.R. and Zehnder, C.M., 1988. Convective partial melting: 1. A model  
963 for the formation of thick basaltic sequences during the initiation of spreading. *Journal of*  
964 *Geophysical Research*, 93, 1031, <https://doi.org/10.1029/JB093iB02p01031>

965 Nirrengarten, M., Mohn, G., Kuszniir, N. J., Sapin, F., Despinois, F., Pubellier, M., ... and  
966 Ringenbach, J. C. (2020). Extension modes and breakup processes of the southeast China-  
967 Northwest Palawan conjugate rifted margins. *Marine and Petroleum Geology*, 113, 104123.

968 Norvick, M.S., and Smith, M.A., 2001, Mapping the plate tectonic reconstruction of southern  
969 and southeastern Australia and implications for petroleum systems: *APPEA Journal*, v. 41,  
970 15–35.

971 Omosanya, K.O., 2020, Cenozoic tectonic inversion in the Naglfar Dome, Norwegian North  
972 Sea: *Marine and Petroleum Geology*, v. 118, 104461.

973 Pérez-Gussinyé, M., and Reston, T. J. (2001). Rheological evolution during extension at  
974 nonvolcanic rifted margins: Onset of serpentinization and development of detachments  
975 leading to continental breakup. *Journal of Geophysical Research: Solid Earth*, 106(B3), 3961-  
976 3975.

977 Pérez-Gussinyé, M., Morgan, J. P., Reston, T. J., and Ranero, C. R. (2006). The rift to drift  
978 transition at non-volcanic margins: Insights from numerical modelling. *Earth and Planetary*  
979 *Science Letters*, 244(1-2), 458-473.

980 Peron-Pinvidic, G., Manatschal, G. and the “IMAGinING RIFTING” Workshop Participants  
981 (2019). Rifted margins: State of the art and future challenges. *Frontiers in Earth Science*, 7,  
982 218.

983 Peron-Pinvidic, G., and Osmundsen, P. T. (2016). Architecture of the distal and outer  
984 domains of the Mid-Norwegian rifted margin: Insights from the Rån-Gjallar ridges system.  
985 *Marine and Petroleum Geology*, 77, 280-299.

986 Peron-Pinvidic, G., Osmundsen, P. T., and Ebbing, J. (2016). Mismatch of geophysical  
987 datasets in distal rifted margin studies. *Terra Nova*, 28(5), 340-347.

988 Pichot, T., Delescluse, M., Chamot-Rooke, N., Pubellier, M., Qiu, Y., Meresse, F., ... and  
989 Auxière, J. L. (2014). Deep crustal structure of the conjugate margins of the SW South  
990 China Sea from wide-angle refraction seismic data. *Marine and Petroleum Geology*, 58, 627-  
991 643.

992 Pietzsch, R., Oliveira, D. M., Tedeschi, L. R., Neto, J. V. Q., Figueiredo, M. F., Vazquez, J.  
993 C. and de Souza, R.S., 2018. Palaeohydrology of the Lower Cretaceous pre-salt lacustrine  
994 system, from rift to post-rift phase, Santos Basin, Brazil. *Palaeogeography,*  
995 *Palaeoclimatology, Palaeoecology*, 507, 60-80.

996 Praeg, D., Stoker, M.S., Shannon, P.M., Ceramicola, S., Hjelstun, B.O., and Mathisen, A.,  
997 2005, Episodic Cenozoic tectonism and the development of the NW European ‘passive’  
998 continental margin: *Marine and Petroleum Geology*, v. 22, 1007–1030.

999 Ranero, C. R., and Pérez-Gussinyé, M. (2010). Sequential faulting explains the asymmetry  
1000 and extension discrepancy of conjugate margins. *Nature*, 468(7321), 294-299.

1001 Reston, T. J. (2005). Polyphase faulting during the development of the west Galicia rifted  
1002 margin. *Earth and Planetary Science Letters*, 237(3-4), 561-576.

1003 Reston, T. (2007). Extension discrepancy at North Atlantic nonvolcanic rifted margins:  
1004 Depth-dependent stretching or unrecognized faulting?. *Geology*, 35(4), 367-370.

1005 Reston, T. J., and Pérez-Gussinyé, M. (2007). Lithospheric extension from rifting to  
1006 continental breakup at magma-poor margins: rheology, serpentinisation and symmetry.  
1007 *International Journal of Earth Sciences*, 96(6), 1033-1046.

1008 Reynolds, S.D., Coblenz, D.D., and Hillis, R.R., 2002, Tectonic forces controlling the  
1009 regional intraplate stress field in continental Australia: results from new finite-element  
1010 modelling: *Journal of Geophysical Research*, v. 107, 10.1029/2001JB000408.

1011 Ritchie, J.D., Johnson, H., and Kimbell, G.S., 2003, The nature and age of Cenozoic  
1012 contractional deformation within the NE Faroe-Shetland Basin: *Marine and Petroleum*  
1013 *Geology*, v. 20, 399-409.

1014 Ritchie, J.D., Johnson, H., Quinn, M.F., and Gatliff, R.W., 2008, The effects of Cenozoic  
1015 compression within the Faroe-Shetland Basin and adjacent areas, in Johnson, H., et al., eds.,  
1016 *The Nature of Compression in Passive Margins: Geological Society, London, Special*  
1017 *Publications*, v. 306, 121–136.

1018 Roberts, D.G. and Schnitker, D. 1984. Initial Reports of the Deep Sea Drilling Project, 81.  
1019 US Government Printing Office, Initial Reports of the Deep Sea Drilling Project  
1020 <https://doi.org/10.2973/dsdp.proc.81.1984>

1021 Rowan, M.G., Peel, F. J., Vendeville, B.C. and Gaullier, V., 2012. Salt tectonics at passive  
1022 margins: Geology versus models–Discussion. *Marine and Petroleum Geology*, 37(1), 184-  
1023 194.

1024 Ryan, W. B., 2009. Decoding the Mediterranean salinity crisis. *Sedimentology*, 56(1), 95-  
1025 136.

1026 Sandiford, M, 2003, Geomorphic constraints on the late Neogene tectonics of the Otway  
1027 Range: *Australian Journal of Earth Sciences*, v. 50, 69–80.

1028 Sandiford, M., Wallace, M., and Coblenz, D., 2004, Origin of the in situ stress field in south-  
1029 eastern Australia: *Basin Research*, v. 16, 325-338.

1030 Sawyer, D.S., Coffin, M.F., Reston, T.J., Stock, J.M. and Hopper, J.R. 2007. COBBOOM:  
1031 the Continental Breakup and Birth of Oceans Mission. *Scientific Drilling*, 5, 13–25,  
1032 <https://doi.org/10.2204/iodp.sd.5.02.2007>

1033 Schoenherr, J., Urai, J.L., Kukla, P.A., Littke, R., Schleder, Z., Larroque, J.-M., Newall, M.J.,  
1034 Al-Abry, N., Al-Siyabi, H.A., Rawahi, Z., 2007. Limits to the sealing capacity of rock salt: a  
1035 case study of the infra-Cambrian Ara Salt from the South Oman salt basin. *AAPG Bull.* 91,  
1036 1541-1557.

1037 Schofield, N., Alsop, I., Warren, J., Underhill, J.R., Lehne, R., Beer, W., Lukas, V., 2014.  
1038 Mobilizing salt: Magma-salt interactions. *Geology* 42, 599-602.

1039 Schofield, N., Holford, S., Millett, J., Brown, D., Jolley, D., Passey, S.R., Muirhead, D.,  
1040 Grove, C., Magee, C., Murray, J. and Hole, M., 2017, Regional magma plumbing and  
1041 emplacement mechanisms of the Faroe-Shetland Sill Complex: implications for magma  
1042 transport and petroleum systems within sedimentary basins: *Basin Research*, v. 29, 41-63.

1043 Sibson, R.H., 1995, Selective fault reactivation during basin inversion: potential for fluid  
1044 redistribution through fault-valve action, in Buchanan J.G., and Buchanan P.G., eds., Basin  
1045 Inversion: Geological Society of London Special Publication 88, 3-19.

1046 Skogseid, J. (2001). Volcanic margins: geodynamic and exploration aspects. *Marine and*  
1047 *Petroleum Geology*, 18(4), 457-461.

1048 Skogseid, J. and Eldholm, O. (1989). Vøring Plateau continental margin: Seismic  
1049 interpretation, stratigraphy, and vertical movements. In Proc. ODP, Scientific Results (Vol.  
1050 104, pp. 993-1030). 10.2973/odp.proc.sr.104.151.1989

1051 Skogseid, J., Planke, S., Faleide, J. I., Pedersen, T., Eldholm, O., and Neverdal, F. (2000). NE  
1052 Atlantic continental rifting and volcanic margin formation. Geological Society, London,  
1053 Special Publications, 167(1), 295-326.

1054 Soares, D. M., Alves, T. M., and Terrinha, P. (2012). The breakup sequence and associated  
1055 lithospheric breakup surface: Their significance in the context of rifted continental margins  
1056 (West Iberia and Newfoundland margins, North Atlantic). *Earth and Planetary Science*  
1057 *Letters*, 355, 311-326.

1058 Stica, J. M., Zalán, P. V., and Ferrari, A. L. (2014). The evolution of rifting on the volcanic  
1059 margin of the Pelotas Basin and the contextualization of the Paraná–Etendeka LIP in the  
1060 separation of Gondwana in the South Atlantic. *Marine and Petroleum Geology*, 50, 1-21.

1061 Stoker, M.S., Hout, R.J., Nielsen, T., Hjelstuen, B.O., Laberg, J.S., Shannon, P.M., Praeg,  
1062 D., Mathiesen, A., van Weering, T.C.E., and McDonnell, A., 2005, Sedimentary and  
1063 oceanographic responses to early Neogene compression on the NW European margin: *Marine*  
1064 *and Petroleum Geology*, v. 22, 1031–1044.

1065 Stoker, M.S., Holford, S.P., Hillis, R.R., Green, P.F., and Duddy, I.R., 2010, Cenozoic post-  
1066 rift sedimentation off northwest Britain: Recording the detritus of episodic uplift on a passive  
1067 continental margin: *Geology*, v. 38, 595-598, doi: 10.1130/G30881.1.

1068 Tassone, D.R., Holford, S.P., Duddy, I.R., Green, P.F. and Hillis, R.R., 2014; Quantifying  
1069 Cretaceous–Cenozoic exhumation in the Otway Basin, southeastern Australia, using sonic  
1070 transit time data: Implications for conventional and unconventional hydrocarbon  
1071 prospectivity: *AAPG Bulletin*, v. 98, 67-117.

1072 Tassone, D.R., Holford, S.P., King, R., Tingay, M.R. and Hillis, R.R., 2017, Contemporary  
1073 stress and neotectonics in the Otway Basin, southeastern Australia, in Turner, J.P., et al., eds.,  
1074 *Geomechanics and Geology: Geological Society, London, Special Publications*, v. 458, p.49-  
1075 88.

1076 Tucholke, B.E., Sibuet, J.-C., Klaus, A., et al., 2004. *Proc. ODP, Init. Repts.*, 210: College  
1077 Station, TX (Ocean Drilling Program). doi:10.2973/odp.proc.ir.210.200

1078 Tugend, J., Manatschal, G., Kusznir, N. J., Masini, E., Mohn, G., and Thinon, I. (2014).  
1079 Formation and deformation of hyperextended rift systems: Insights from rift domain mapping  
1080 in the Bay of Biscay-Pyrenees. *Tectonics*, 33(7), 1239-1276.

1081 Tugend, J., Gillard, M., Manatschal, G., Nirrengarten, M., Harkin, C., Epin, M. E. and  
1082 Mcdermott, K. (2020). Reappraisal of the magma-rich versus magma-poor rifted margin  
1083 archetypes. *Geological Society, London, Special Publications*, 476(1), 23-47.

1084 Ulvrova, M. M., Brune, S., and Williams, S. (2019). Breakup without borders: how  
1085 continents speed up and slow down during rifting. *Geophysical Research Letters*, 46(3),  
1086 1338-1347.

1087 Van Hinsbergen, D. J., Maffione, M., Koornneef, L. M., and Guilmette, C. (2019). Kinematic  
1088 and paleomagnetic restoration of the Semail ophiolite (Oman) reveals subduction initiation  
1089 along an ancient Neotethyan fracture zone. *Earth and Planetary Science Letters*, 518, 183-  
1090 196.

1091 Warren, J.K., 2017. Salt usually seals, but sometimes leaks: implications for mine and cavern  
1092 stability in the short and long term. *Earth-Science Rev.* 165, 302-341.

1093 White, R. S., Smith, L. K., Roberts, A. W., Christie, P. A. F., and Kusznir, N. J. (2008).  
1094 Lower-crustal intrusion on the North Atlantic continental margin. *Nature*, 452(7186), 460-  
1095 464.

1096 White, R. and McKenzie, D. 1989. Magmatism at rift zones: the generation of volcanic  
1097 continental margins and flood basalts. *Journal of Geophysical Research*, 94, 7685,  
1098 <https://doi.org/10.1029/JB094iB06p07685>

1099 Whitmarsh, R. B., Beslier, M. O., and Wallace, P. J. (1998). Leg 173. In *Proc. ODP, Init. Rep*  
1100 (Vol. 173, p. 493).

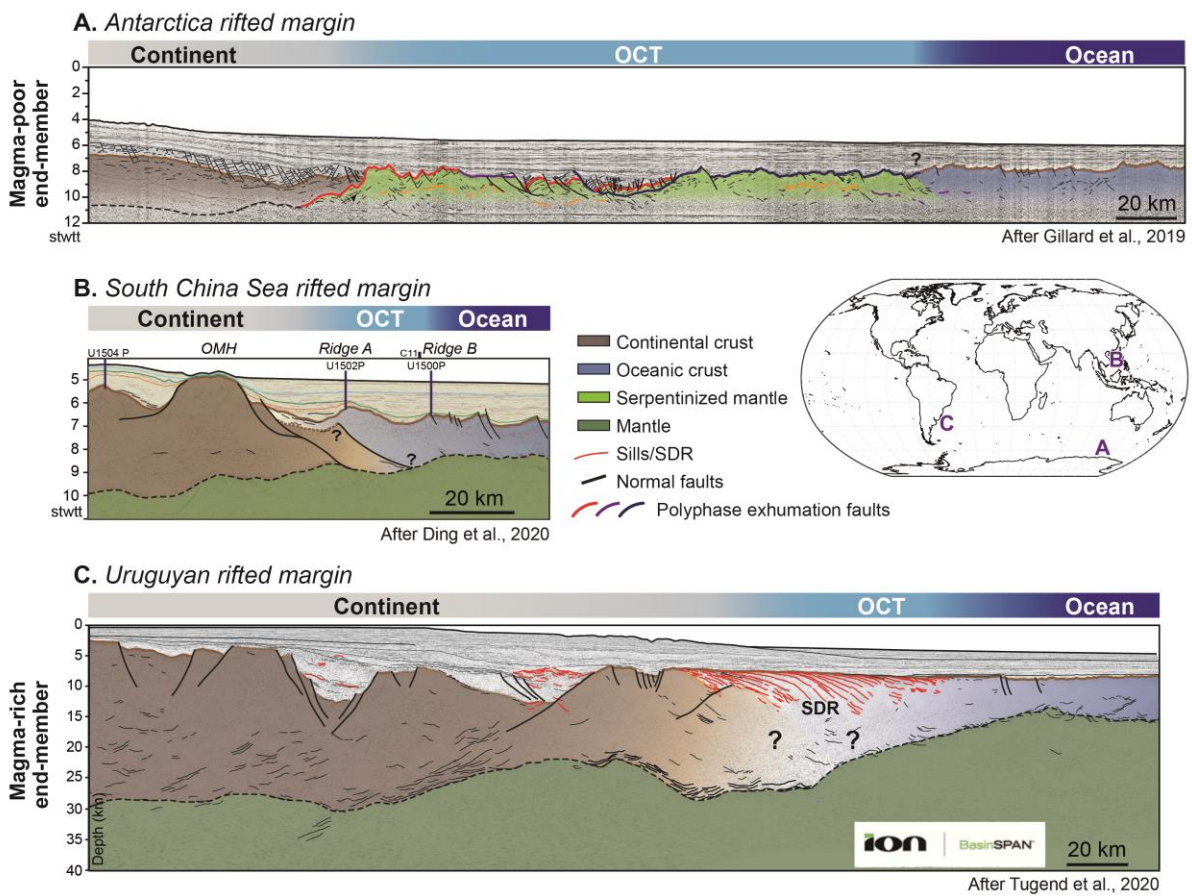
1101 Whitmarsh, R. B., Minshull, T. A., Russell, S. M., Dean, S. M., Louden, K. E., and Chian, D.  
1102 (2001). The role of syn-rift magmatism in the rift-to-drift evolution of the West Iberia  
1103 continental margin: geophysical observations. *Geological Society, London, Special*  
1104 *Publications*, 187(1), 107-124.

1105 Zhuo, Q. G., Meng, F. W., Zhao, M. J., Li, Y., Lu, X. S., and Ni, P., 2016. The salt chimney  
1106 effect: delay of thermal evolution of deep hydrocarbon source rocks due to high thermal  
1107 conductivity of evaporites. *Geofluids*, 16(3), 440-451.

1108 Ziegler, P.A., Cloetingh, S., and van Wees, J.D., 1995, Dynamics of intra-plate  
 1109 compressional deformation: the Alpine foreland and other examples: Tectonophysics, v. 252,  
 1110 7–59.

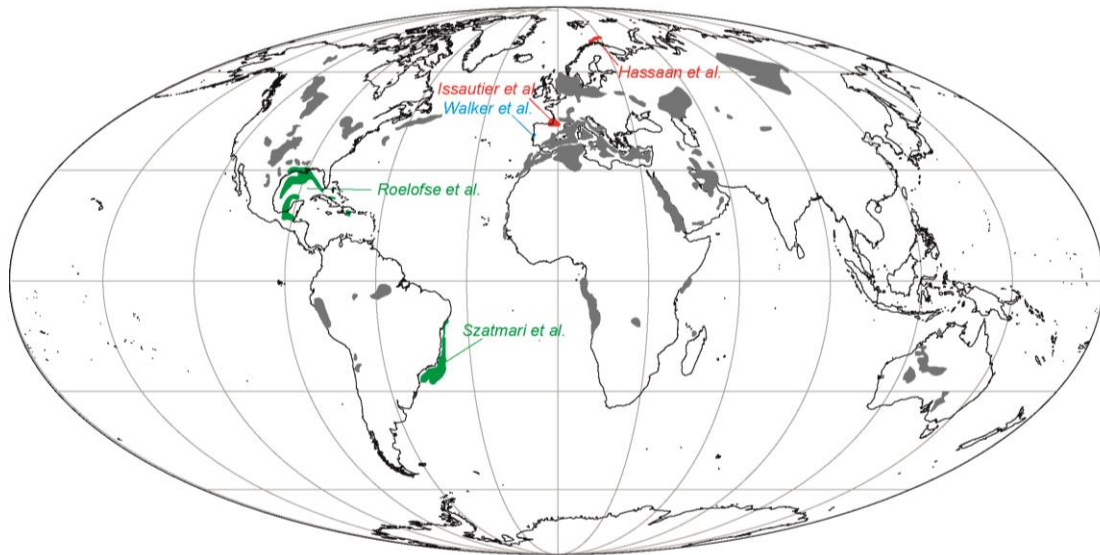
1111

1112 **Figures**



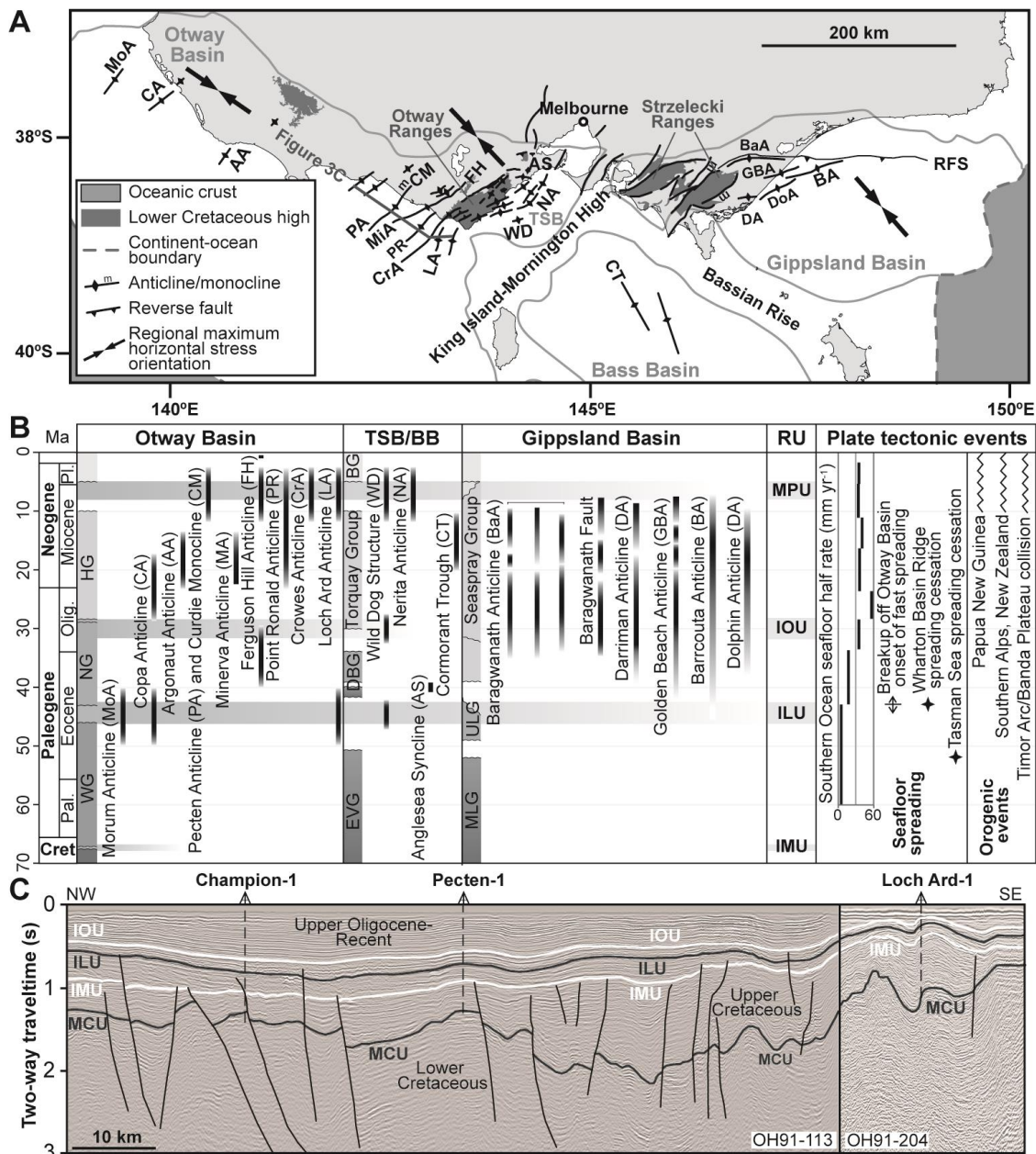
1113

1114 Figure 1. Reappraisal of the magma-poor versus magma-rich rifted margin archetypes  
 1115 (Tugend et al., 2020). Worldwide examples show a wide spectrum of Ocean Continent  
 1116 Transitions (OCT) geometries and continental breakup magmatism. A. Antarctica rifted  
 1117 margin (after Gillard et al., 2019) B. South China Sea rifted margin (Ding et al., 2020) C.  
 1118 Uruguayan rifted margin (after Tugend et al., 2020).



1119

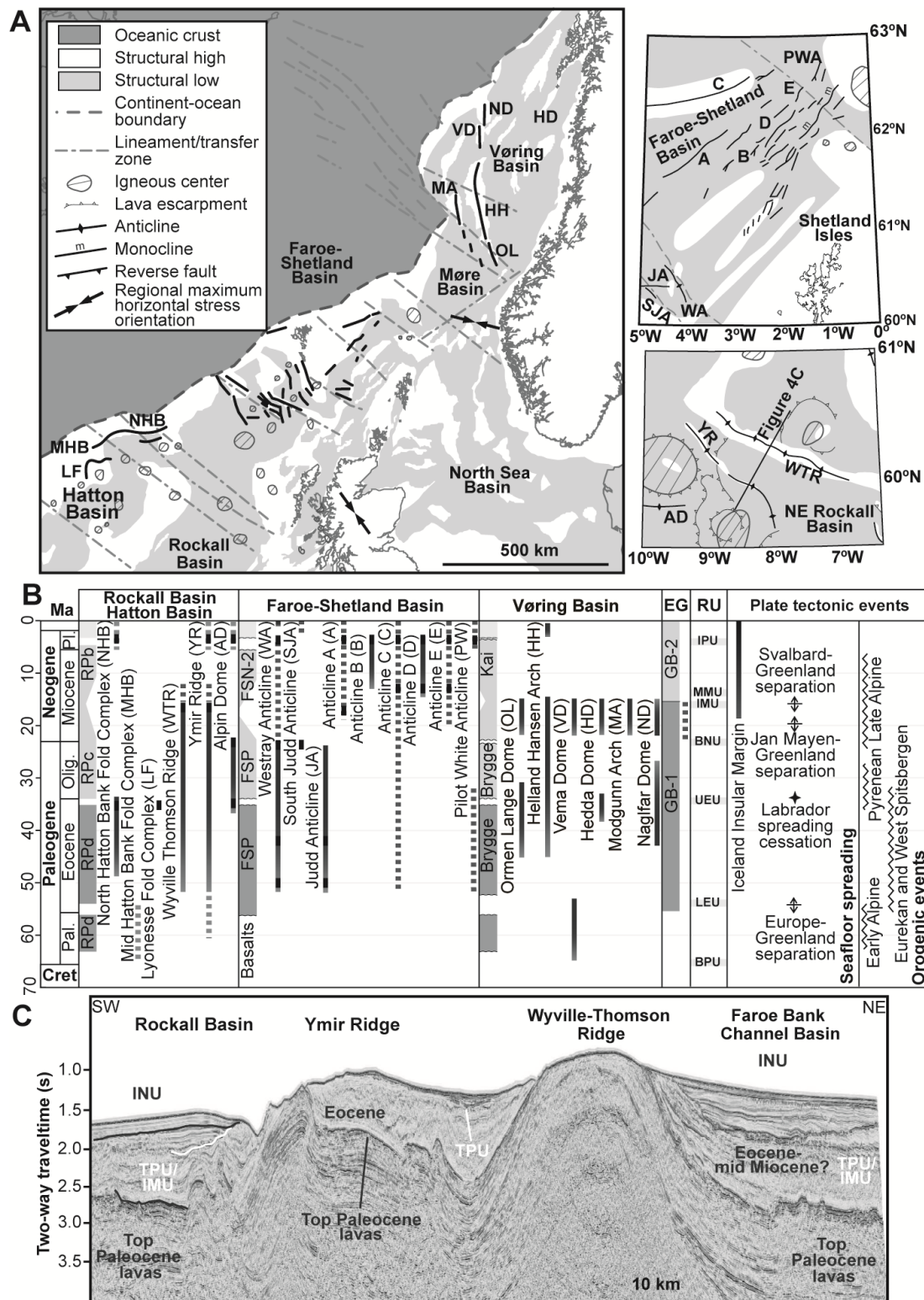
1120 Figure 2. Worldwide distribution of main salt basins (areas in grey), modified after Hudec  
 1121 and Jackson (2007). The case studies in this special volume, which are located on salt bearing  
 1122 basins, are highlighted on the map and colour coded according to their geodynamic context:  
 1123 red for syn-rift basins, blue for cratonic basins, and green for passive margin basins.



1124

1125 Figure 3. (a) Distribution of post-breakup structures along the basins of the southern  
 1126 Australian margin. Strikes of the majority of structures are orthogonal to present-day stress  
 1127 orientations. The Otway and Strzelecki Ranges are inliers of Lower Cretaceous sediments  
 1128 formed during post-breakup compression and uplift. BB, Bass Basin; RFS, Rosedale Fault  
 1129 System; TSB, Torquay sub-basin. (b) Chronologies of post-breakup fold growth along the  
 1130 southern Australian margin, in relation to regional stratigraphy and plate tectonic events.

1131 Constraints on fold growth in the Otway, Torquay and Bass basins based on Holford et al.  
1132 (2014) and Mahon and Wallace (2020) for the Gippsland Basin. ILU, intra-Lutetian  
1133 unconformity; IMU, intra-Maastrichtian unconformity; IOU, intra-Oligocene unconformity;  
1134 MCU, mid-Cretaceous unconformity; MPU, Miocene-Pliocene unconformity; RU, regional  
1135 unconformities. (c) Seismic reflection profile from the Otway Basin, southern Australian  
1136 margin, showing multiple low-amplitude post-breakup anticlines. Intensity of folding  
1137 increases towards the Otway Ranges in the SE. Folding of IOU and overlying sediments  
1138 attests to near-continuous late Oligocene-Pliocene folding, whilst thinning of early Paleogene  
1139 sequence bound by IMU and ILU witnesses mid-late Eocene deformation.



1140

1141 Figure 4. (a) Distribution of post-breakup structures along the basins of the NW European  
 1142 margin (modified after Ritchie et al. (2008)). Inset maps show distribution of structures in the

1143 Faroe-Shetland Basin (above) and North Rockall Basin (below). See (b) for acronyms. (b)  
1144 Chronology of post-breakup fold growth along the NW European and conjugate east  
1145 Greenland margin, in relation to regional stratigraphy and plate tectonic events. Constraints  
1146 on fold growth based on Doré et al. (2008), Lundin and Doré (2002), Johnson et al. (2005),  
1147 Ritchie et al. (2003, 2008), Stoker et al. (2005). Regional unconformities based on Praeg et  
1148 al. (2005) and Stoker et al. (2005), and plate tectonic events based on Doré et al. (2008),  
1149 Lundin and Doré (2002) and Stoker et al. (2010). BPU, base Paleogene unconformity, BNU,  
1150 base Neogene unconformity; EG, East Greenland, IMU, intra-Miocene unconformity; IPU,  
1151 intra-Pliocene unconformity; LEU, lower Eocene unconformity; MMU, mid-Miocene  
1152 unconformity; RU, regional unconformities; UEU, upper Eocene unconformity. (c) Seismic  
1153 reflection profile from the North Rockall Basin imaging the Wyville Thomson Ridge (axial  
1154 trace ~200 km, amplitude ~2 km, wavelength ~40 km). TPU, top Paleogene unconformity.  
1155 Thinning of Eocene-mid Miocene succession on NE flank of the structure provides evidence  
1156 for near-continuous growth of this fold during these times (Ritchie et al., 2008).